GOLD-CORE SILVER-SHELL NANOPARTICLE AS A SERS SUBSTRATE FOR THE DETECTION OF PESTICIDES IN TEA

A Thesis

presented to

the Faculty of the Graduate School

at the University of Missouri-Columbia

In Partial Fulfillment

of the Requirements for the Degree

Master of Science

---

by

Kairui Zhai

Dr. Mengshi Lin, Thesis Supervisor

JULY 2023

The undersigned, appointed by the dean of the Graduate School, have examined the thesis entitled

GOLD-CORE SILVER-SHELL NANOPARTICLE AS A SERS SUBSTRATE FOR THE DETECTION OF PESTICIDES IN TEA

presented by Kairui Zhai,
a candidate for the degree of Master of Science
and hereby certify that, in their opinion, it is worthy of acceptance.

Dr. Mengshi Lin, Food Science

Dr. Andrew D. Clarke, Food Science

Dr. Liqun Gu, Biological and Biomedical Engineering

ACKNOWLEDGEMENTS

I would like to express my sincere gratitude to my advisor, Dr. Mengshi Lin, for the numerous opportunities he provided, his unwavering support, and his willingness to engage in research discussions during my master's studies. The specialized training program played a pivotal role in cultivating my skills and boosting my research confidence. I would like to extend my heartfelt appreciation to my committee members, Dr. Clarke and Dr. Gu, for their invaluable time and dedicated efforts throughout the year. Their insightful advice, professional guidance, and wealth of knowledge have greatly contributed to my understanding of scientific research. I am grateful to all the individuals I had the pleasure of working with over the past two years. In particular, I would like to express my heartfelt gratitude to Lin Sun for not only providing me with an enlightening introduction to the research but also for generously dedicating her time to help me become familiar with my own research. Lastly, I deeply appreciate my parents, my mom Yijun Wang, my father Jiong Zhai, and my stepfather, Yi Wei - for their unwavering love and support throughout my graduate studies. I am especially grateful to my mom, whose presence and encouragement were instrumental in reaching this significant milestone. Without her, this achievement would not have been attainable.

TABLE OF CONTENTS

LIST OF FIGURES

LIST OF TABLES

GOLD-CORE SILVER-SHELL NANOPARTICLE AS A SERS SUBSTRATE FOR THE DETECTION OF PESTICIDES IN TEA

Kairui Zhai

Dr. Mengshi Lin, Thesis Supervisor

In recent years, there has been significant interest in the application of innovative analytical methods combined with nanomaterials for the rapid detection of food contaminants. Pesticides are commonly used in tea cultivation to protect tea plants from various pests and diseases. However, pesticide residues can contaminate tea and have negative impacts on the environment and human health. Conventional chromatography-based analytical methods are destructive and require lengthy sample preparation. In this study, gold-silver core-shell nanoparticles (Au/Ag) coupled with surface-enhanced Raman spectroscopy (SERS) were developed as a novel, facile, and sensitive testing technique for detecting pesticide residues in tea samples.

The Ag coating of Au NPs can continuously enhance Raman scattering signals. To assess the effectiveness of SERS method, a Raman reporter molecule, known as 4-aminothiophenol, was employed. This approach resulted in distinctive Raman spectra like fingerprints, and the SERS method demonstrated an impressive sensitivity capable of detecting concentrations as low as 0.1 mg/L. Two pesticides, phosmet and paraquat, were successfully detected individually or as a mixture in tea samples by SERS coupled with nanosubstrate. Strong Raman scattering signals for both phosmet and paraquat were obtained within a Raman shift range of 400–2000 cm^{-1}.

The contamination of grapes with pesticide residues has generated significant concern. As consumers demand safer food products, it has become essential to conduct regular pesticide residue inspections in food. The objective of the second study was to synthesize polyhedral gold nanostars (AuNS) with multi-angled corners and utilize them in conjunction with SERS to detect pesticide residues in grape products. This study aimed to develop a fast and simple technique for detecting two pesticides (phosmet and paraquat) present on the surface of grapes using SERS. During the experiment, ethanol was applied to the contaminated grape surface extract pesticides. Subsequently, AuNS were introduced to generate SERS signals of the pesticides. The spiky tips of the AuNS act as SERS hot-spots, amplifying the Raman signals of the analyte molecules. Furthermore, the rough surface of AuNS increases the surface area, resulting in improved interactions between the substrate and analyte.

Prominent SERS peaks of blended contaminants were observed under a 785 nm laser excitation, and these peaks were chosen to characterize and quantify the concentration of the contaminants. It was discovered that the SERS intensity of these two peaks changed in proportion to the concentration ratio of phosmet and paraquat. Additionally, AuNS demonstrated better SERS enhancement performance than gold nanoparticles. Our experimental results indicate that the lowest detectable concentration for both pesticides on grape surfaces is 0.5 ppm. These findings suggest that SERS coupled with AuNS is a practical and highly promising approach for the detection and quantification of trace contaminants in food.

CHAPTER 1

INTRODUCTION

1.1 Background

In recent years, there has been growing apprehension regarding food safety, driven by widely publicized incidents involving the accidental or intentional addition of contaminants to food. Food contamination is indeed a grave concern due to the elevated levels of chemicals found in food products, which pose significant health risks. Safeguarding the public from the detrimental effects of contaminated food has become an increasingly challenging endeavor. Therefore, reducing these risks and ensuring the safety of the food supply chain is of paramount importance to protect public health.

Eating contaminated food imposes a substantial global health burden, with approximately 600 million individuals, nearly 1 in 10 people worldwide, falling ill as a result. Tragically, this leads to an estimated 420,000 deaths annually, causing a significant loss of 33 million healthy life years, as measured by Disability-Adjusted Life Years (DALYs). These statistics highlight the urgent need for comprehensive efforts to enhance food safety and prevent the adverse impacts of foodborne illnesses. Moreover, unsafe food in low- and middle-income countries has dire economic consequences, resulting in an estimated annual loss of US$110 billion in productivity and medical expenses (Food safety, 2022). This significant financial toll underscores the urgency of implementing effective measures to ensure food safety, protect public health, and mitigate the economic impact of foodborne illnesses in these regions.

Pesticides play an essential role in food production, serving to control various pests that can jeopardize crops and food quality. They are utilized to manage insects, rodents, weeds, bacteria, mold, and fungus, ensuring the integrity and yield of agricultural produce. By effectively controlling these pests, pesticides contribute to maintaining the overall safety and abundance of food resources. However, pesticides are also potentially toxic to humans inducing adverse health effects such as cancer, reproductive issues, and impacts on the immune or nervous systems (Food safety, 2022). As early as 1990, a task force of the World Health Organization (WHO) estimated that approximately one million unintentional pesticide poisonings occur annually, resulting in approximately 20,000 deaths (Boedeker et al., 2020).

For example, on July 16, 2013, a tragic incident occurred in the village of Dharmashati Gandaman in the Saran district of Bihar, India. At least 23 students lost their lives, and many others fell ill after consuming a midday meal that was contaminated with pesticides. Subsequent investigations revealed that the cooking oil used in the meal had been stored in a container previously used for insecticides. The cooking oil was found to contain dangerously high levels of monocrotophos, an agricultural organophosphate pesticide known for its toxicity (Reddy & Colman, 2017).

Data on pesticide exposure were obtained from calls to Poison Control Centers (PCCs) reported by the American Association of Poison Control Centers. In the United States, pesticides are associated with a significant number of deaths posing a considerable public health concern. On average, there are 23 pesticide-related deaths reported annually. Additionally, poison control centers receive an average of 130,136 calls between 2006 and

2010, with approximately 17.8% (20,116 cases) requiring treatment in healthcare facilities each year.

According to the Agency for Healthcare Research and Quality (AHQR), there were an average of 7,385 emergency room visits per year from 2006 to 2008 and 1,419 hospitalizations annually from 2005 to 2009. Considering emergency department visits, hospitalizations, and deaths, the estimated annual national cost associated with pesticide exposures is nearly $200 million USD. It's important to note that this cost does not include factors such as lost work time, hospital physician fees, or pesticide-induced cancers. These statistics highlight the significant economic and health burden caused by pesticide exposure (Langley & Mort, 2012).

Food safety issues have existed for a considerable period and are not limited to the present time. Furthermore, given the rapid transportation and distribution of food across various countries, the repercussions of such incidents have a global reach. Consequently, it becomes crucial for food inspectors and regulators to arrive promptly at the location to conduct on-site inspections and analyze the contaminants present in the food. Hence, there is an urgent need within the food industry for dependable, rapid, and straightforward technology that enables on-site detection and analysis.

High-performance liquid chromatography (HPLC) and gas chromatography (GC) are considered benchmark techniques for analyzing chemical contaminations. These methods are frequently supplemented with other techniques like UV-visible spectroscopy, nuclear magnetic resonance (NMR), or mass spectrometry (Donno et al., 2020). While these methods offer satisfactory specificity and sensitivity, they do have some limitations. These limitations include intricate and time-consuming sample preparation processes, the

requirement for skilled personnel, and challenges associated with large-scale screening. Consequently, there is a crucial need to establish uncomplicated, fast, portable, and highly sensitive methods specifically designed for applications within the food industry.

In recent years, significant attention has been given to the rapid advancement of nanotechnology, which primarily revolves around the characterization, fabrication, and manipulation of structures that possess at least one dimension ranging from 1 to 100 nanometers. Within this context, SERS has emerged as a novel and remarkably sensitive analytical technique. SERS relies on the utilization of nanoscale SERS substrates to achieve enhanced electromagnetic and chemical enhancements of Raman scattering signals, thereby enabling highly sensitive detection and analysis. Gold and silver nanoparticles are the most commonly employed SERS-active substrates.

These nanoparticles typically have a size (diameter) ranging from 10 to 100 nm. In the case of electromagnetic enhancement, the free electrons present on the surface of these metal nanoparticles can interact with magnetic fields, giving rise to surface plasmon oscillations via resonance (Panigrahi et al., 2007). As a result of these interactions, robust enhancements in the surface electromagnetic field occur, leading to significant amplification of the Raman signals emitted by the analyte molecules. Core-shell nanoparticle and gold nanostar coupled with SERS have received much attention as novel technology for qualitative and quantitative analysis of chemical compounds. The combination of coreshell nanoparticles and gold nanostars with SERS has garnered substantial interest as a novel technology for the qualitative and quantitative analysis of chemical compounds.

1.2 Objectives

The study aimed to achieve the following objectives: 1. Develop and evaluate the SERS method coupled with gold-core silver-shell substrates (Au/Ag) for the detection of pesticide residues in tea; 2. Synthesize polyhedral gold nanostars (AuNS) with multi-angled corners and develop a SERS method coupled with AuNS for the detection of pesticide residues in grapes.

CHAPTER 2

LITERATURE REVIEW

2.1 Surface-enhanced Raman Spectroscopy

Raman scattering, named after CV Raman and his student KS Krishnan who first observed it in 1928, became renowned in the field. In recognition of their discovery, Raman was awarded the Nobel Prize for the technique in 1930 (C.V. Raman The Raman Effect - Landmark, 1998). Today, Raman spectroscopy is widely used in analytical chemistry to identify various materials, such as gases, liquids, and solids, by analyzing their specific chemical functional groups. It operates on the principle of light interacting with the chemical bonds within a substance. When laser light interacts with molecular vibrations, phonons, or other excitations in the system, the energy of the laser photons is shifted either up or down. This energy shift provides information about the vibrational modes present in the material (Hassing, 2019).

However, spontaneous Raman scattering is typically weak. As depicted in Figure 2-1, when Raman scatters a light source onto a sample, the molecule is excited to a virtual state. The virtual state is not an actual energy level but represents the energy of the laser at that moment, and the molecule remains in this transient state briefly. Once in the virtual state, the light can be scattered back, returning the molecule to its ground state (known as Rayleigh scattering). However only a small fraction of the scattered photons (typically 1 in 1 million) can undergo an excitation, resulting in scattered photons with frequencies different from and usually lower than those of the incident photons (Harris & Bertolucci, 1989). Therefore, the stability of the light source and its intensity greatly impact the

applicability of normal Raman spectroscopy in chemical analysis, particularly when compared to faster and less expensive infrared spectroscopy.

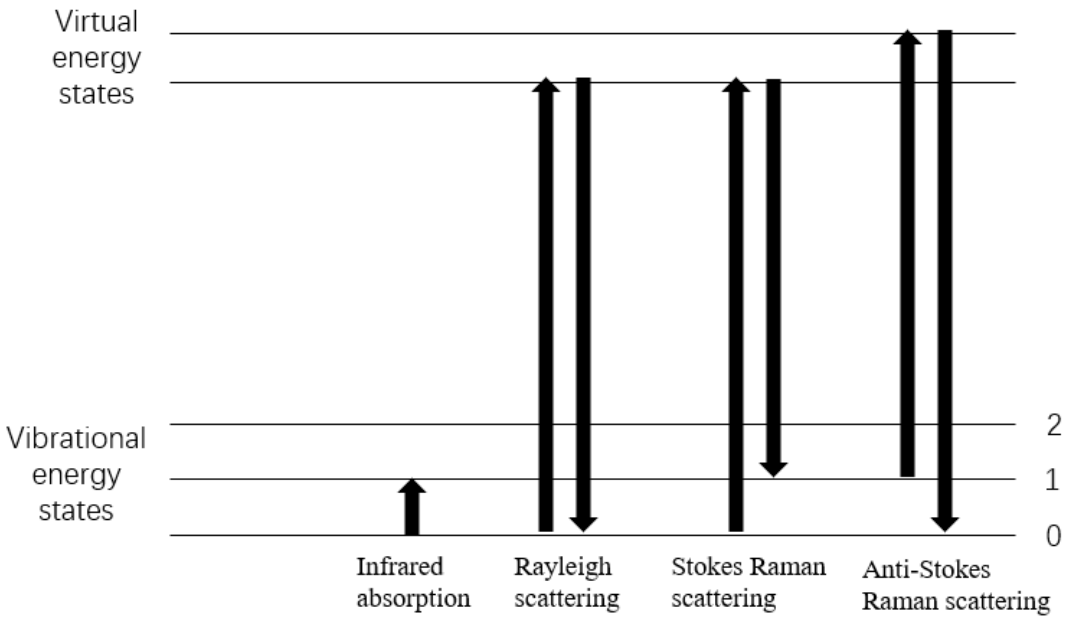

Figure 2-1 Energy-level diagram showing the states involved in Raman spectra.

SERS was first discovered by Fleischmann et al. in 1974 (Pilot et al., 2019). It is a surface-sensitive technique that amplifies Raman scattering signals emitted by molecules adsorbed on roughened metal surfaces (Figure 2-2), such as gold, silver, and copper, or by nanostructures like gold, silver, and Au/Ag. SERS allows for the collection of Raman scattering signals from analyte molecules, providing vibrational information akin to a fingerprint. The enhancement factor in SERS can surpass 10^6, enabling the detection of single molecules using this technique (Xu et al., 2013).

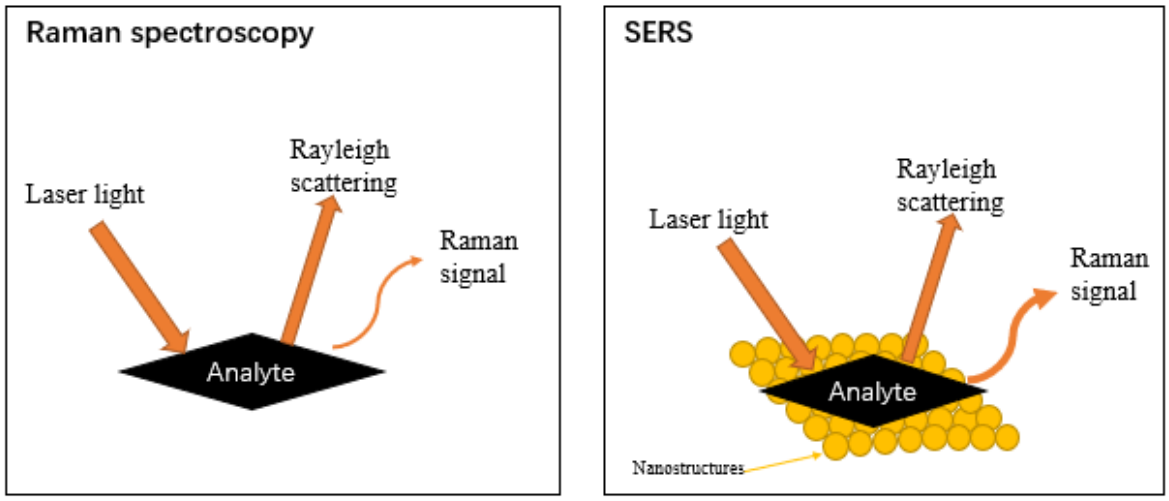

Figure 2-2 Schematic illustration of the difference between Raman spectroscopy and SERS.

SERS has two main enhancement mechanisms: electromagnetic and chemical effects (Stöckle et al., 2000). The electromagnetic effect stems from the heightened electric field strength experienced by the analyte due to the interaction between the metal surface and the excitation light. Notably, localized surface plasmon resonance (LSPR) plays a crucial role in this effect. LSPR arises when the collective oscillation of valence electrons within a coinage metal nanoparticle resonates with the frequency of the incident light (Kim et al., 2015). Chemical enhancement in SERS involves resonance Raman scattering, wherein new electronic excitations of adsorbed molecules act as resonant intermediate states. Unlike electromagnetic enhancement, chemical enhancement has a limited range and is closely associated with the properties of the analyte molecules themselves.

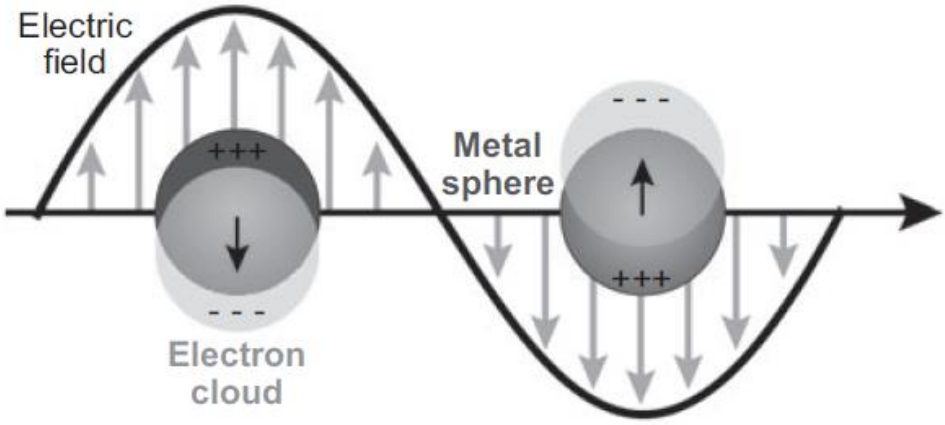

Figure 2-3 Illustration of the localized surface plasmon resonance effect (Sun et al., 2016).

2.2 Gold and silver nanoparticles

Gold and silver nanoparticles are commonly used in SERS due to their distinctive characteristics. Gold nanoparticles are particularly favored in SERS because of their unique attributes (Altunbek et al., 2016). When illuminated by light, they exhibit LSPR which occurs when conduction electrons synchronize their movement, resulting in enhanced Raman scattering, by precisely adjusting the size, shape, and composition of gold nanoparticles, the LSPR can be finely tuned to maximize Raman signal enhancement (Kim et al., 2015). The interaction of light with gold nanoparticles generates strong electric fields near their surfaces, creating localized regions called "hot-spots." These intensified electromagnetic fields greatly amplify the Raman signals of nearby molecules, thereby enhancing the sensitivity of SERS. Additionally, gold nanoparticles possess exceptional chemical stability, making them resistant to oxidation and ensuring consistent and reliable SERS performance over time.

Silver nanoparticles also play a prominent role in SERS due to their distinctive properties. Similar to gold nanoparticles, silver nanoparticles exhibit LSPR, resulting in

intensified electromagnetic fields on their surfaces (Loiseau et al., 2019). Through precise control of size, shape, and composition, the LSPR of silver nanoparticles can be tailored to optimize SERS enhancement. Importantly, silver nanoparticles typically offer higher enhancement factors compared to gold nanoparticles, owing to the stronger electromagnetic field enhancements near their surfaces (Deriu et al., 2023). This characteristic enables greater amplification of Raman signals from analyte molecules. Additionally, the plasmonic properties of silver nanoparticles make them sensitive to the excitation wavelength used in SERS. By carefully selecting an appropriate excitation wavelength, resonance conditions can be met, thereby maximizing the SERS enhancement (Li et al., 2010).

2.3 Gold-core silver-shell nanoparticles (Au/Ag)

Au/Ag nanoparticles are employed in SERS to amplify the Raman scattering signals of molecules. These nanoparticles comprise a gold core surrounded by a silver shell, which synergistically offers distinctive optical and electromagnetic properties, highly advantageous for SERS applications. The gold core serves as a stable and inert support, while the silver shell enhances the electromagnetic field near the nanoparticle surface (Ghosh Chaudhuri & Paria, 2012). This means Au/Ag nanoparticles enhance the Raman scattering signals of molecules in SERS by utilizing the stable gold core and the silver shell's ability to amplify the electromagnetic field near the nanoparticle surface.

This enhancement occurs due to the localized LSPR effect, where incident light induces collective oscillations of conduction electrons in the nanoparticle. The LSPR effect in silver generates strong electromagnetic fields around the nanoparticle surface, leading to increased interaction between the incident light and nearby molecules. When a molecule

of the sample comes in close proximity to an Au/Ag nanoparticle, the electromagnetic field amplifies the Raman scattering signal of the molecule, the silver shell's strong electromagnetic field enhances the Raman signal, allowing for more sensitive detection and identification of molecules in SERS (Bhattacharjee et al., 2018).

In summary, Au/Ag nanoparticles are used in SERS to enhance the Raman scattering signals of molecules through the LSPR effect generated by their unique structure. This enables highly sensitive molecular detection and analysis in various fields such as chemistry, biochemistry, and materials science.

Gold-core silver-shell nanoparticles (Au/Ag) enhance the Raman scattering signals of molecules in SERS by using the stable gold core and the silver shell's ability to amplify the electromagnetic field near the nanoparticle surface (Yilmaz & Yilmaz, 2020). This amplification arises from the LSPR effect, which induces strong electromagnetic fields that enhance the interaction between incident light and nearby molecules, and the enhanced Raman signal, facilitated by the silver shell's electromagnetic field, enables sensitive detection and identification of molecules in SERS, benefiting various fields including chemistry, biochemistry, and materials science (Haynes et al., 2005).

2.4 Gold nanostar (AuNS)

Currently, there is significant interest in complex three-dimensional (3D) metal nanostructures due to their optical properties resulting from intricate surfaces with multi-angled corners. Among these structures, AuNS, a non-symmetric and non-sharply edged 3D nanostructure, possesses a central core and multiple protruding branching angles (Lin et al., 2021). The presence of these sharp edges and branching angles renders AuNS highly

sensitive to local dielectric environments, exhibiting exceptional surface-enhanced Raman scattering (SERS) effects.

The optical properties of gold nanomaterials, including AuNS, are largely influenced by factors such as size, shape, and aggregate structure (Njoki et al., 2007). Hence, the preparation of metal nanoparticles with diverse morphologies is crucial for their optimal performance in SERS. AuNS have gained significant attention in SERS applications due to their distinctive optical properties, tunability, and high enhancement factors. They find use in various fields such as analytical chemistry, biosensing, surface science, and biomedical research, where highly sensitive and selective molecular detection and identification are crucial.

AuNS serves as nanostructures in SERS to amplify molecular Raman scattering signals. Their complex surface morphology creates multiple LSPR hot-spots, leading to a remarkable enhancement of the electromagnetic field near the nanoparticle surface (Sun et al., 2019). This augmented field, generated by the collective oscillation of conduction electrons induced by incident light, significantly amplifies the Raman scattering signals of adjacent molecules (Lin et al., 2021). The exceptional SERS performance of AuNS stems from their unique design, characterized by sharp branches and intricate surface roughness. These branches create numerous hot-spots, increasing the likelihood of molecule-nanoparticle interactions and enhancing the sensitivity and signal amplification capabilities of SERS.

2.5 Surface-enhanced Raman spectroscopy applied to food safety

In the 21st century, there has been a growing focus on food safety and public safety, people necessarily need to develop a simple, efficient, and effective detection method in

the field of detection technology. SERS has emerged as such a method, offering efficiency, rapidity, and convenience for the quantitative and qualitative detection of chemical contaminants in food samples (Li et al., 2014). These contaminants primarily include agricultural and environmental pollutants like pesticides, herbicides, heavy metals, and toxins. SERS holds significant advantages for food safety applications, particularly in its ability to provide rapid on-site analysis, allowing for quick screening of food samples to ensure food safety (Xu et al., 2022). SERS also finds use in the authentication and quality control of food products, as it can analyze unique Raman spectral fingerprints of specific compounds or components, verifying their quality (Xu et al., 2022).

CHAPTER 3

GOLD-CORE SILVER-SGELL NANOPARTICLE AS A SERS SUBSTRATE FOR THE DETECTION OF PESTICIDES IN TEA

3.1 Introduction

Tea, which has its origins traced back to China around 2700 BC, stands as one of the most widely consumed beverages worldwide. Throughout history, it has evolved from a medicinal brew made by boiling fresh leaves in water to a daily refreshment. Tea cultivation and processing practices began in the 3rd century CE (Sinnathurai, 2023). Based on the processing techniques employed, three primary tea variants emerged: non-fermented tea, exemplified by green tea; semi-fermented tea, such as oolong tea; and fermented tea, black tea. It has been discovered that tea leaves contain substances beneficial to human health, such as polyphenols and flavonoids (Lin et al., 2021). However, tea leaves may also contain potentially harmful substances, such as pesticide residues resulting from their use in tea cultivation.

Pesticides are essential in agriculture for increasing crop production, preventing plant diseases, and improving farmers' profits (Cooper & Dobson, 2007). Various types of pesticides are regularly used in agricultural production. These residual pesticides in food products can be toxic to humans, causing short-term adverse health effects as well as chronic adverse effects that may occur months or years after exposure (Pesticides & Human Health | Californians for Pesticide Reform, n.d.).

Paraquat is a fast-acting, nonselective contact herbicide that is absorbed by the foliage and has some translocation in the xylem. It is commonly used for broad-spectrum control of broad-leaved weeds and grasses in fruit orchards and plantations, as well as for

inter-row weed control in various crops (Lock & Wilks, 2001). While paraquat is permitted for use in over 100 countries worldwide, it's highly toxic to humans. Paraquat catalyzes the formation of reactive oxygen species (ROS), particularly superoxide radicals, through redox cycling, resulting to extensive cell injury, necrosis, and a secondary inflammatory reaction (Enhanced Elimination of Poisons - ClinicalKey, n.d.).

On the other hand, organophosphorus pesticides (OPs), such as phosmet, are widely used agricultural pesticides due to their broad-spectrum insecticidal activity, high efficacy, and low cost. Phosmet, a phthalimide-derived, non-systemic, organophosphate insecticide, is mainly used on apple trees or tea crops to control codling moths. However, phosmet has toxicological effects, and its residues can pose significant harm to human health (Good et al., 1993). Because tea has a shorter interval between pesticide treatment and harvest compared with other crops (Abd El-Aty et al., 2014), it represents a substantial potential source of pesticide residue exposure, especially for habitual tea drinkers.

To solve this issue, it is important to monitor pesticide residues in tea to minimize the potential ingestion of these harmful pesticides. There are several traditional techniques for the detection and measurement of pesticide residues in tea, such as liquid chromatography-high-resolution mass spectrometry (Saito-Shida et al., 2018), ultrahigh-performance liquid chromatography-tandem mass spectrometry (Zhang et al., 2010), gas chromatography-mass spectrometry (GC–MS) (L. Chen et al., 2012).

However, these methods have certain drawbacks, such as being laborious, tedious, and involving complex sample pre-treatment. The extraction and identification of trace levels of analyte molecules in samples is a difficult task in the detection of pesticides in complex food matrices (tea, vegetable, etc.). SERS is a sensitive, label-free, and non-

destructive analytical technique, which can amplify Raman signals by over 10^6 times the ordinary level. By utilizing innovative nanosubstrates, SERS has emerged as a new analytical method that has proven useful in the food industry for the rapid detection of pesticide residues in agricultural products.

SERS techniques rely on SERS-active substrates to amplify Raman signals. Among various types of nanoparticles, gold-core silver-shell (Au/Ag) nanoparticles have garnered significant attention in recent years. This is due to the outstanding stability, sensitivity, and versatility of silver and gold, the two most widely used materials for SERS-active substrates (Sharma et al., 2012). However, single-element nanoparticles, such as gold nanoparticles (Au NPs) or silver nanoparticles (Ag NPs), have limited plasmonic absorptions. It is believed that the continuous enhancement of Raman signals can be achieved by coating Au NPs with Ag. The silver shell boasts excellent optical and electrical properties that make it ideal for achieving satisfactory results in SERS measurement (Awiaz et al., 2023). This stability of the gold core and the properties of the silver shell make Au/Ag NPs promising for chemical and biological sensing applications (Stamplecoskie et al., 2011).

Tea is composed of various compounds, including catechins, chlorophyll, caffeine, amino acids, and polyphenols (Lin et al., 2021). Unfortunately, most of these compounds have strong fluorescence signals that can significantly interfere with the detection of pesticide in tea using Raman spectroscopy. Furthermore, the quantity of pesticide residues in tea is usually very low and their Raman signals are correspondingly weak. Although SERS has the potential to increase the Raman intensity and simultaneously suppress fluorescence signals, the weak information about pesticides in tea can be overwhelmed by

high-concentration components in tea, making it difficult to analyze pesticide information. Therefore, the objective of this study was to develop novel SERS methods coupled with sensitive Au/Ag nanoparticles to detect pesticide residues in green tea.

3.2 Materials and Methods

3.2.1 Materials

Hydrogen tetrachloroaurate solution ($HAuCl_4$, 30 wt% in dilute HCl), silver nitrate (ACS reagent $\geq$ 99.9%), L-ascorbic acid, paraquat (Pestanal® analytical standard), phosmet (Pestanal® analytical standard), 4-aminothiophenol (4-ATP), activated charcoal (10 - 12 mesh) were obtained from Sigma-Aldrich (St. Louis, MO, USA). Trisodium citrate dihydrate (certified ACS), iron (III) oxide, 99.9% (metals basis), water (HPLC grade), and acetone (HPLC grade) were purchased from Fisher Scientific (Fair Lawn, New Jersey, USA). Green tea was purchased from a local grocery store. A filter device (Whatman) with 0.2 μm polyethersulfone (PES) membrane was used for sample preparation. All chemicals were used as received without further purification, and HPLC water was used throughout the experiments. Prior to use, all glassware were soaked in aqua regia (HCl/HNO_3 3:1, v/v) for 24 h and rinsed with HPLC water.

3.2.2 Synthesize of Au/Ag substrate

Firstly, gold colloids as seeds were synthesized based on the $HAuCl_4$-citrate reduction method (Xie et al., 2009). HPLC water (90 mL) in an Erlenmeyer flask was heated to the boiling temperature at 100ºC, then 10 mL of gold solution (17.3 μL of $HAuCl_4$, 30 wt% in dilute HCl + 10 mL water) was added. After the solution was boiled again, 4 mL of 0.25% sodium citrate (0.1 g sodium citrate dihydrate + 40 mL water) was added into a flask. The solution was stirred continuously until it turned a red wine color, following

which the heating ceased while the stirring was allowed to proceed for an additional 30 minutes.

Next, 6 mL of L-ascorbic acid (0.1 mol/L, 0.889 g L-ascorbic acid + 50 mL water) and as-prepared Au seeds were mixed in a 50 mL glass beaker and stirred continuously. A volume (13.5 mL) of $AgNO_3$ solution (0.01 mol/L, 85.7 mg + 50 mL water) was added drop by drop into the above beaker with continuous stirring to form Au/Ag NPs. As the silver shell formed, the color of the Au/Ag colloids changed from red to cream.

3.2.3 Characterization of Au/Ag NPs

The absorbance of the gold seed solution was measured using a UV-1099i spectrophotometer (Shimadzu, Kyoto, Japan) across the wavelength range of 400 to 700 nm. A cuvette filled with deionized water was used as a blank. Thermo Scientific Spectra 300 (S)TEM coupled with the Super-X system was used to view the shape and analyze the elemental composition of core-shell nanoparticles. An aliquot (5 μL) of Au/Ag solution was dropped on a copper grid prior and dried prior to the STEM analysis.

3.2.4 Preparation of standard solutions and green tea samples

The following solutions were prepared: 4-aminothiophenol standard solution (0, 0.01, 0.05, 0.1, 0.5, 1, and 2 mg/kg), paraquat solution (0, 0.1, 0.5, 1, 2, 5, 10, and 20 mg/kg), and phosmet solution (0, 0.1, 0.5, 1, 2, 5, 10, and 20 mg/kg). 4-ATP were used as the Raman probe to measure the enhancement of Au/Ag NPs. The solvent for both 4-minothiophenol and the paraquat standard solutions was water. Acetone was the solvent for the phosmet standard solution. A solvent solution without any pesticides was used as the control.

A 2.5 g tea bag was placed into water boiling at 100°C for a duration of three minutes. The membrane filter was used to purify the green tea. Iron oxide (3200 mg) and activated charcoal (1200 mg) were added to a 40 mL centrifuge tube, then 40 mL of the above tea samples was added. The mixture was vortexed thoroughly, shaking for 12 h, followed by centrifugation at 2700 RCF or 5500 RPM for 5 min. A colorless supernatant was obtained, extracting the supernatants from the mixture, and spiked with different amounts of paraquat, phosmet to make various concentrations of two pesticides samples (0, 0.1, 0.5, 1, 2, 5, 10, and 20 mg/kg).

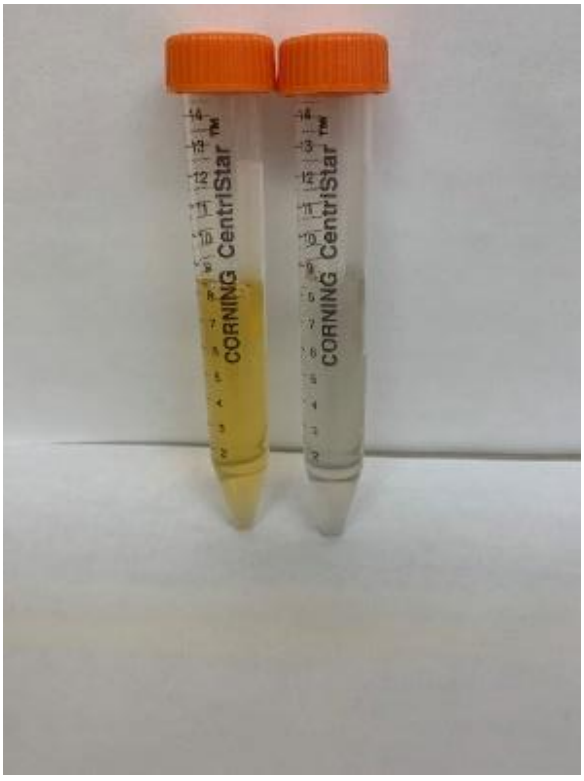

Figure 3-1 Green tea (left) and green tea after pretreatment (right).

3.2.5 SERS measurement

The prepared Au/Ag NPs were used to measure phosmet and paraquat in the green tea samples. An aliquot (5 μL) of the sample solution and 5 μL of Au/Ag NPs were mixed and

deposited on a gold-coated slide. Before SERS measurement, the droplet was dried on a 35 °C hot plate to evaporate water. In this study, a DXR2 Raman spectroscopy equipped with a 785-nm laser source (Thermo Fisher Scientific Inc., Madison, WI, USA) was used.

All data were collected in the range of 400–2000 cm^{-1} using a ×10 objective lens and 25-μm pinhole aperture. The final spectrum was averaged from 10 spectra scanned from different locations on each sample, with 1 second of exposure time every scan, 3 seconds of exposure time for sample collection, and 20 mW of laser power. Ten measurements were averaged for each sample concentration. 4-ATP was selected as a probe molecule to evaluate the SERS effect of the Au/Ag substrate.

3.2.6 Raman spectral data analysis

Originlab (Originlab Corporation, Northampton, Massachusetts, United States) and Delight software (Delight, D-squared Development Inc., LaGrande, OR, USA) was utilized for Raman spectral analyses. Partial least squares (PLS) analysis was used in analyzing the SERS spectral data. First, spectral data were pre-processed by smoothing at 2 cm^{-1} and a second-derivative transformation with 12 cm^{-1} gap was employed to eliminate instrumental noises and separate overlapping peaks and adjust the baseline shift to reduce spectral noise. For the prediction of analyte concentrations, PLS models were developed. The correlation coefficient, r, was used to assess how accurately the PLS model predicts the analyte concentrations. The *r* values range from 0 to 1, with values close to 1 indicating a strong positive linear relationship. Ten replicate measurements were conducted for each sample and their average value was used in the calibration plot. The following equation was used to calculate the root mean squared error of prediction (RMSEP). RMSEP is a typical measure of prediction error utilized in statistical modeling.

$$\text{RMSEP}=\sqrt{\frac{\sum(y_i-\hat{y})^2}{n}} \quad (1)$$

The y_i represents the actual concentration, $\hat{y}$ represents the predicted concentration created by the model, and n represents the number of samples. The ratio of performance to deviation (RPD) is the ratio of sample standard deviation to the prediction error. The smaller the prediction error, the greater the RPD (Lin et al., 2021). Thus, a higher RPD signifies a better prediction model, and a value of RPD greater than 5 is satisfactory for quality control (Williams & Sobering, 1993). Greater r and RPD and lower RMSEP indicate a model with a higher ability for prediction.

Analytical enhancement factor (AEF):

The analytical enhancement factor (AEF) of the SERS method using Au/Ag NP as the SERS substrate was calculated by measuring SERS signals of 10 μL of 4-ATP solution with and without having Au/Ag NPs as the substrate deposited onto a gold-coated microscope slide. The AEF of the SERS technique was determined using the following formula:

$$\text{AEF} = I_{SERS} / I_{RS} \times C_{RS} / C_{SERS} \quad (2)$$

Where I_{SERS} and I_{RS} indicate the peak intensities in SERS and normal Raman spectra, respectively, and the analyte concentrations in SERS and normal Raman measurements are indicated by C_{SERS} and C_{RS}, respectively.

3.3 Results & discussion

3.3.1 Characterization of synthesized Au/Ag Nps

Fig. 3-1A shows the seed solution containing Au/Ag NPs, which exhibits a wine-red color due to its ability to reflect red light and absorb green light. Fig. 3-1B shows the UV-visible spectrum acquired from the seed solution, resulting from the surface plasmon resonance (SPR) activities of AuNPs. The characteristic peak at 530 nm, which is indicative of no agglomeration or precipitation in the AuNP solution and a monodisperse distribution of nanoparticles, is due to SPR occurring on the surface of AuNPs (Chen et al., 2020). It is possible to use the highest absorbance peak of the seed solution as a rapid check to ensure that the seed solution has been synthesized correctly.

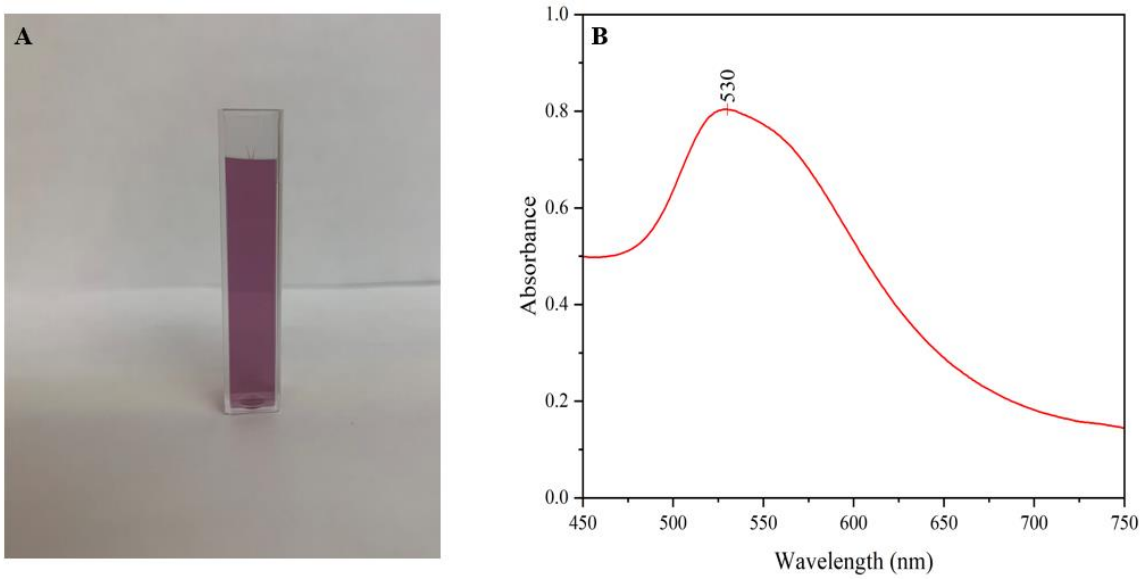

Figure 3-2 The seed solution for Au/Ag NPs (A) and a UV-Vis spectrum of the seed solution (B).

Au/Ag NPs were created through a two-step seed-growth procedure. In the first step, Au cores were synthesized by reducing $HAuCl_4$ with trisodium citrate in an aqueous solution. Subsequently, the Ag shell gradually formed and grew, coating the Au cores after

mixing $AgNO_3$ and ascorbic acid (used as a reducing agent and stabilizer) solutions with Au NP colloid (Asgari et al., 2020). EDS images displayed homogeneous core-shell structures for the synthesized nanoparticles (Fig. 3-2A), and most of the synthesized Au/Ag NPs were spherical in shape with a narrow size range. Furthermore, STEM imaging provided additional evidence of the core-shell structure of the nanoparticles (Fig. 3-2B), revealing a brighter Au core and a dark Ag shell due to the difference in atomic numbers.

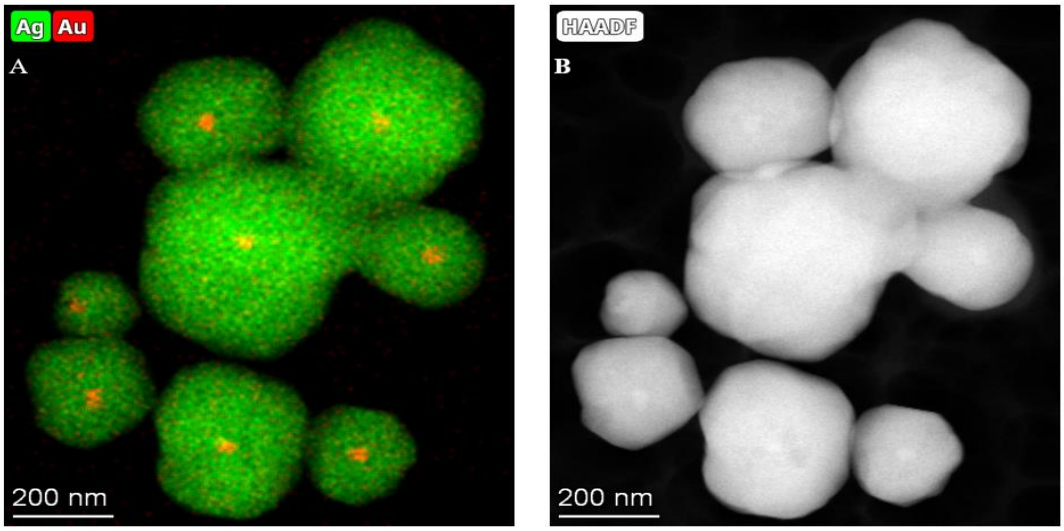

Figure 3-3 EDS image of Au/Ag NPs (A) and the corresponding STEM image (B).

3.3.2 Evaluation of SERS performance of Au/Ag NPs

To evaluate the SERS performance of the Au/Ag NPs substrate, various concentrations of 4-ATP were measured. 4-ATP is an aromatic thiol, and the self-assembly of silver and gold nanoparticles was linked with 4-ATP to create a metal-molecule-metal sandwich architecture that was characterized by SERS under an off-SPR condition (Hu et al., 2007). Fig. 3A shows the SERS spectra of 10 mg/L of 4-ATP, showing three prominent Raman peaks located at 1074, 1178, and 1587 cm^{-1}. Fig. 3B depicts Raman spectra of SERS using Au/Ag NP substrates modified by a 4-ATP solution with different ratios (0 – 2 mg/L).

The intensity of the typical spectral bands decreased as the adsorbent concentration dropped from 2 to 0 mg/L, but the Raman signals were still detectable even at concentrations as low as 0.01 mg/L, indicating the high quality and sensitivity of Au/Ag NPs as SERS substrates.

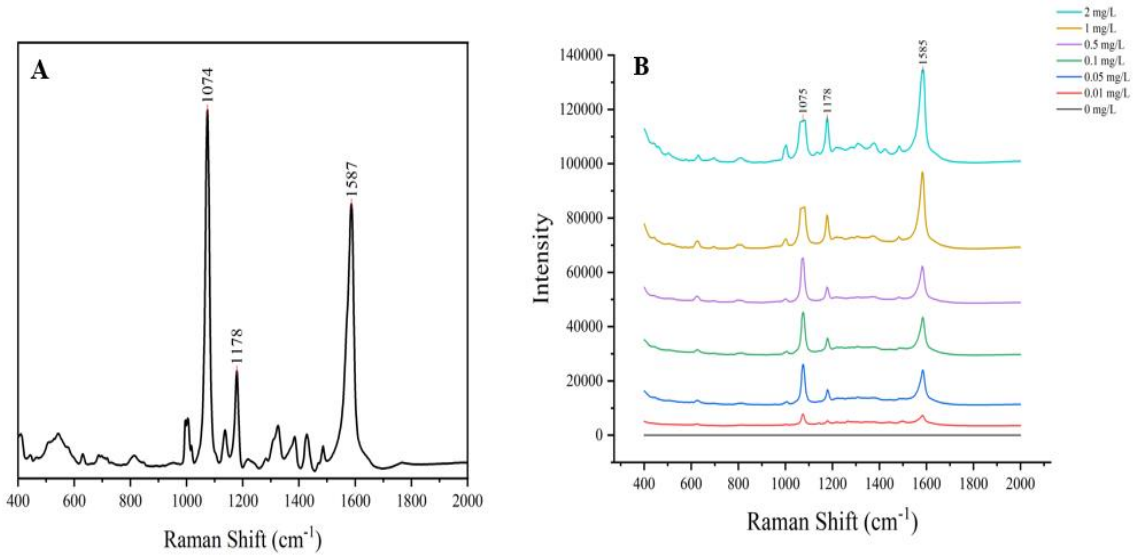

Figure 3-4 Average Raman spectra (n=10) of the 10 ppm 4-ATP solution (A); average Raman spectra (n=10) of different concentrations of 4-ATP solution (B).

3.3.3 Determination of paraquat, phosmet and their mixture in water and green tea

Paraquat (1,1′dimethyl-4,4′-bipyridinium dichloride) is a quaternary ammonium compound that is positively charged and independent of the pH value of the solution (Shackman et al., 2015). The high hydrophilicity and ionic nature of paraquat enable the molecules to be strongly adsorbed on the Ag shells via hydrogen, ionic, and π bonds (Luo et al., 2018). Fig 3-5A shows representative SERS spectra (n=10) of standard paraquat solutions (0.1 - 20 mg/L).

Due to the interactions between analyte molecules and the surfaces of Au/Ag NPs, four major characteristic peaks were identified in relation to the conventional Raman spectra of paraquat: C–N stretching at 837 cm^{-1}, the C=N bending at 1190 cm^{-1}, the C–C

structural distortion at 1292 cm^{-1}, and the C=N stretching at 1647 cm^{-1} (Lin et al., 2021). The spectral peak observed at 1647 cm^{-1} is considered the most distinctive feature in the paraquat spectrum and serves as a reliable indicator for detecting the presence of paraquat in tea samples. However, as evident from Fig. 3-5A, all peaks are distinctly discernible at all paraquat solution concentrations examined. An increase in paraquat concentration from 0 to 20 mg/L resulted in an intensity of approximately 6000.

A two-step seed-growth procedure was utilized to create Au/Ag NPs, which were used to detect phosmet in an acetone-water solution. Fig. 3-5B presents the average SERS spectra (n = 10) for phosmet samples of various concentrations. The "fingerprint-like" Raman peaks are located at 501, 604, 771, 1012, and 1448 cm^{-1}. The intensity of the Raman spectra for phosmet molecules increased significantly from 0 to 20 mg/L. The peak at 501 cm^{-1} corresponds to the rocking vibration of CH_2 and PO_2 (Costa et al., 2012). A peak at 604 cm^{-1} corresponds to stretching vibrations of the C–S bond (Liu et al., 2012), while the Raman peak at 771 cm^{-1} arises from the S–C bond and in-plane bending of C=N in the ring (Luo et al., 2016). Additionally, the Raman peak at 1012 cm^{-1} arises from the asymmetric stretching of P–O–C and a Raman peak at 1448 cm^{-1} is due to the bending of the C–H bond (Fan et al., 2014). The Raman shift bands at 501 and 771 cm^{-1} are clearly visible, major peaks are observable at all concentrations of phosmet, including 0.1 mg/L, and very high intensities are observed for all concentrations of pesticide solutions indicating that "fingerprint-like" Raman signals can be utilized to identify phosmet in the acetone-water solution.

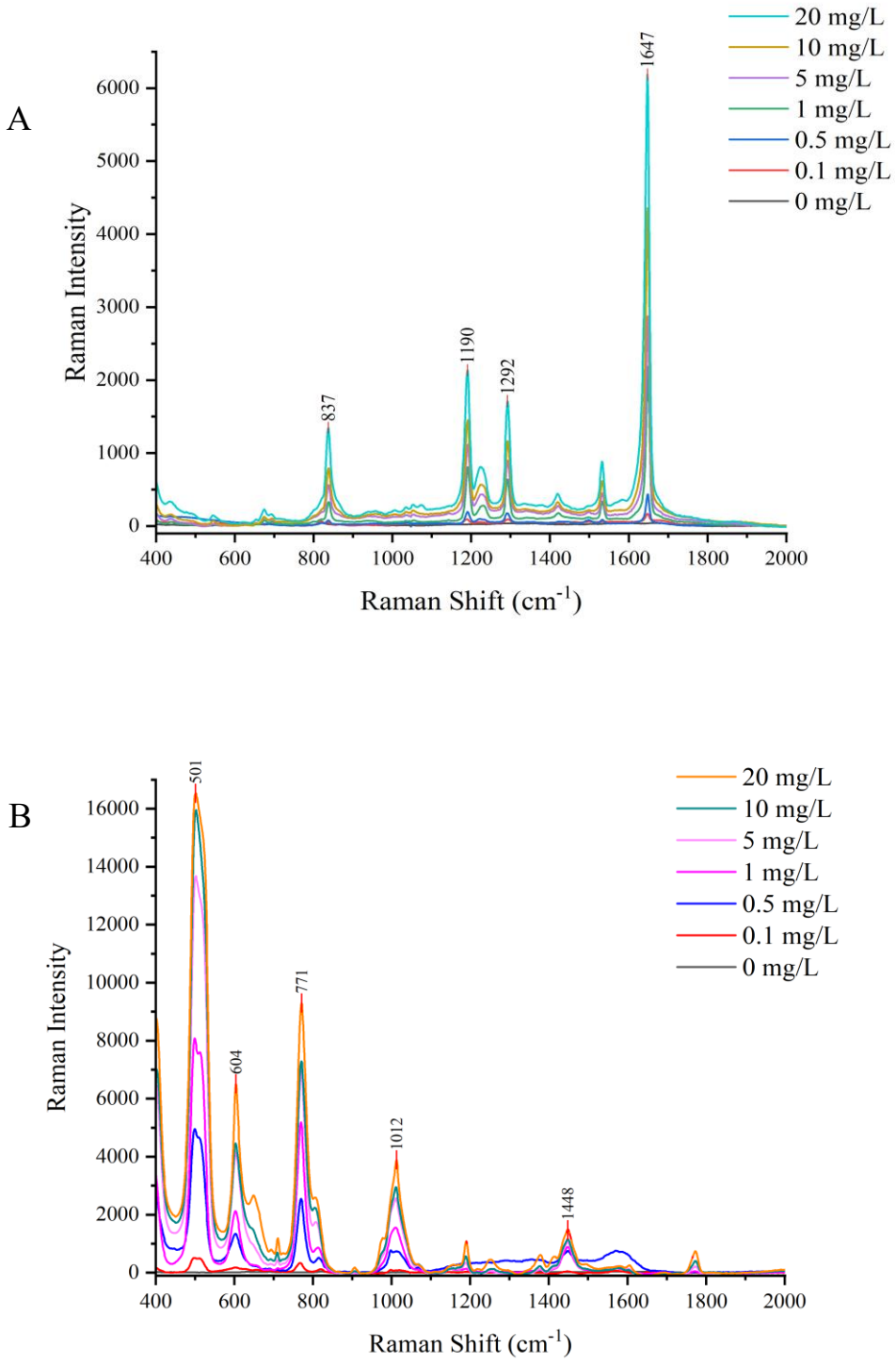

Figure 3-5 Averaged SERS spectra of different concentrations of paraquat aqueous solutions (A); averaged SERS spectra of different concentrations of phosmet aqueous solutions (B).

Tea is a widely consumed beverage and a significant agricultural commodity globally. There are three types of tea that are extensively consumed: black tea, green tea, and oolong tea. The degree of oxidation distinguishes these three kinds of tea. Black tea is fully oxidized, green tea is slightly oxidized, and oolong tea falls between black and green tea in terms of oxidation. Due to its minimal degree of processing, green tea retains more polyphenols than the other two types (Lin et al., 2021). However, tea can be contaminated by various pesticides. Residues of pesticides have been detected in tea bags, which pose a hidden danger to tea consumers and cause great concern about the potential health effects of pesticide exposure. The 2018 report by European Food Safety Authority (EFSA) found that more than 15% of the tested teas contained pesticide residues above the corresponding MRLs (EFSA et al., 2020).

As a nonselective herbicide, paraquat can be used to control weeds in tea cultivation. The Codex Alimentarius, an international guideline and the basis for regulations in many countries, has set the maximum residue level (MRL) for paraquat in tea at 0.2 mg/L. Phosmet is a pesticide that is frequently used to control various types of crop pests. MRLs in China for phosmet in cereals, fruits, and vegetables are limited to 0.5, 0.5, and 5 mg/L, respectively (Chen et al., 2020). The current tolerance level for phosmet residue in dried tea leaves is set at 7 ppm in the United States (EPA). In addition, both phosmet and paraquat have toxicological effects, and their residues can pose significant health risks to humans. This study evaluated the SERS performance of Au/Ag NPs in real-food samples using green tea spiked with different amounts of paraquat and phosmet mixture.

The average (n = 10) SERS spectra of various concentrations of the mixture are shown in Fig. 3-6A. The characteristic peaks of phosmet can be observed at 502, 604, 770,

1011, and 1448 cm^{-1}, while for paraquat, the characteristic peaks are located at 1189, 1295, and 1650 cm^{-1}. The intensity of Raman peaks increased as the mixture concentration increased from 0 to 20 mg/L. Fig. 3-6B displays the averaged (n = 10) SERS spectra of the tested samples from green tea containing both pesticides. “Fingerprint-like” Raman peaks for phosmet are located at 501, 602, 768, 1009, and 1447 cm^{-1}, while for paraquat, the characteristic peaks are located at 1188, 1293, and 1647 cm^{-1}.

The spectra show a positive correlation between mixture concentrations and Raman intensities as Raman shift wavenumbers increase as the concentration of the mixture in green tea samples increases from 0 to 20 mg/kg. Compared to the mixture (Fig. 3-6A), although different components in the green tea extract (such as pigment, polyphenols, and caffeine) contributed more noise to the Raman spectra, no significant interfering noise appeared in these spectra.

Even at low concentrations, all characteristic peaks of each pesticide were clearly distinguishable and only slightly shifted, which also indicates that other compounds in green tea were removed by the sample pretreatment method. Our SERS measurements indicate that the intensity of characteristic peaks corresponds to different concentrations of phosmet and paraquat in tea and can be used to quantify pesticide residues in real-food samples.

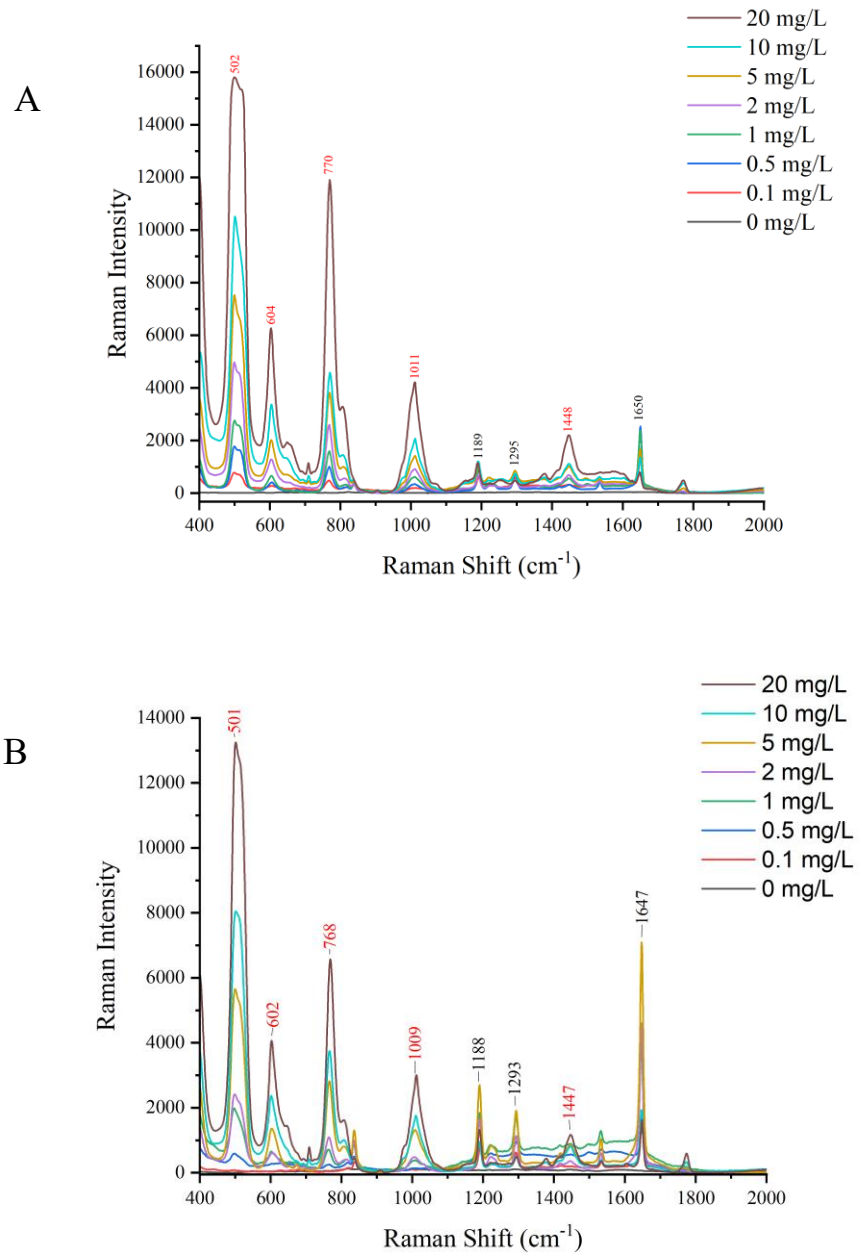

Figure 3-5 Averaged SERS spectra of different concentrations of mixture solutions (A); averaged SERS spectra of different concentrations of mixture in green tea (B).

The R value and RMSEP for the data are 0.98 and 1.38 mg/L, respectively (Fig. 3-6). The high R value indicates a strong linear correlation between the actual and predicted concentrations. To ensure accuracy, ten measurements were taken at randomly selected

spots for each sample concentration. The calculations yielded an AEF of 10^4, suggesting a significant interaction between pesticide molecules and gold nanostars. Consequently, as the pesticide concentration increases, the Raman signals also increase, demonstrating the effectiveness of the proposed method. The results highlight the reproducibility of this approach, indicating its reliability. Therefore, the SERS method using gold nanostars as substrates exhibits excellent performance and holds promise for future applications.

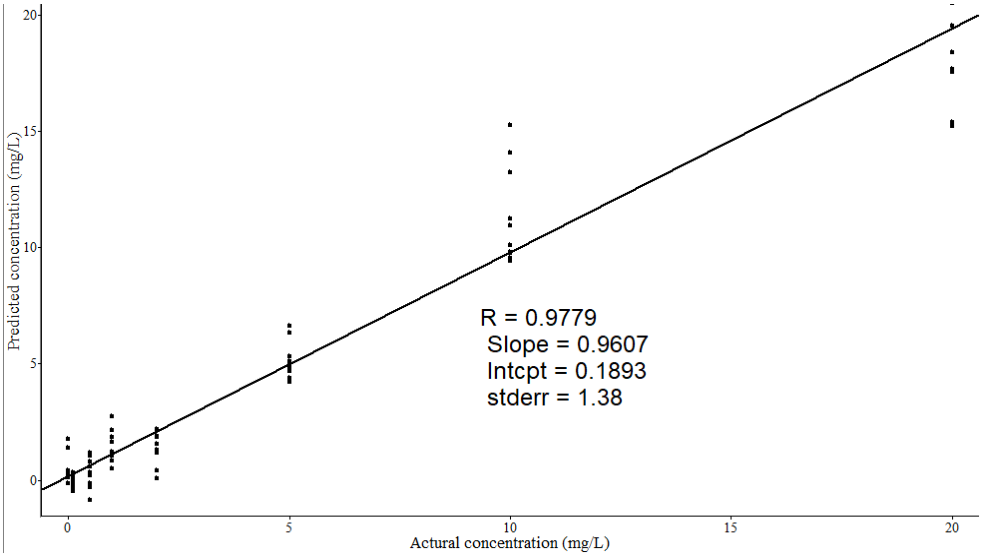

Figure 3-6 Prediction of paraquat and phosmet concentration in green tea using the PLS model.

Table 3-1 Band assignment of major peaks for phosmet and paraquat

Raman shift (cm^{-1})	**Tentative assignment**
501	Rocking vibration of CH_2 and PO_2
602	Stretching vibrations of C-S
768	S-C and in-plane bending of C=N in ring
1009	Asymmetric stretching of P-O-C
1188	C=N bending
1293	C–C structural distortion
1447	Bending of C-H
1647	C=N stretching

3.4 Conclusion

This research has established a dependable and effective SERS substrate based on Au/Ag NPs for qualitative and quantitative analysis of phosmet and paraquat mixture in green tea. The detection of phosmet and paraquat as a mixture in green tea demonstrated the outstanding detection performance of Au/Ag NPs. PLS analyses indicate that SERS coupled with Au/Ag NPs can detect the pesticide mixture in green tea samples with a low concentration of 0.1 mg/kg. Real food analysis using SERS combined with Au/Ag NPs is facile and repeatable. SERS shows promise as a technique for detecting pesticides at trace levels. However, it is challenging to use SERS to detect residual compounds in complex food matrices because their SERS spectra are affected by many factors, such as nanosubstrates and food. Thus, further study is needed to design substrates, improve the extraction procedure, and evaluate various food items.

CHAPTER 4

RAPID DETECTION OF MUTI-PESTICIDES RESIDUES ON GRAPES USING THE SERS TECHNIQUE

4.1 Introduction

Pesticides play a crucial role in agricultural production for safeguarding crops and produce against pests and diseases. However, as the agricultural industry increasingly relies on a wide range of pesticides to protect crops and produce, concerns about the health risks associated with pesticide residues are growing. The improper use of pesticides, including overuse, misuse, and the mixing of multiple pesticides, poses potential risks not only to human health but also to the environment and ecology (Zhang et al., 2014). Moreover, previous research indicates that pesticide residues are easily found in many food products (Narenderan et al., 2020). Various reports suggest that intake of different pesticides with different modes of action carries risk, as continuous exposure to pesticides can lead to depression, neurological deficits, diabetes, respiratory diseases such as rhinitis, and in extreme cases, cancer, fetal death, spontaneous abortion, and genetic diseases (Ntzani et al., 2013).

Substrates play an important role in SERS techniques by facilitating significant Raman enhancements. One promising biosensing strategy for molecular detection is localized surface plasmon resonance (LSPR) (Hutter & Fendler, 2004). LSPR relies on surface plasmons that are tightly confined to metallic nanoparticles and exhibits, high sensitivity to changes in the dielectric environment surrounding the particles. This unique property has been harnessed to detect molecular targets when they bind to nanoparticle surfaces (Park et al., 2015). Noble metal nanospheres, such as silver (Ag) and gold (Au),

are the most commonly used materials for LSPR applications, owing to their well-established synthetic methods and plasmon resonance properties at visible wavelengths (Lu et al., 2009).

SERS is a powerful analytical tool for the detection, quantification, and identification of chemical and biological samples. SERS has advantages over traditional detection methods, including high-performance liquid chromatography (HPLC) and gas chromatography-mass spectrometry (GC-MS). SERS rapid acquisition of molecular "fingerprints" of analyte molecules, and multiple Raman spectra can be collected from samples in a short amount of time (Liu et al., 2013). There is a growing interest in utilizing SERS for detecting trace amounts of pesticides, and its detection sensitivity continue to improve through the use of better substrates and optimized methods. The SERS effect can reach a level of more than 10^6 and the limit of detection can be as low as a single molecule or parts per billion (μg/L) level (Mulvihill et al., 2008; Radziuk & Moehwald, 2015).

Among these substrates, gold nanostars (AuNS) have gained much attention due to their intricate polyhedral structures. These nanostars, which have multiple angled corners and rough surfaces, exhibit unique optical properties. AuNS are three-dimensional (3D) nanostructures with an asymmetrical and multi-edged shape, consisting of a central core and several branching angles protruding from it (Sun et al., 2019). The sensitivity of AuNS to local dielectric environments can be attributed to the "tip effect" or "lightning rod effect", which arise from the presence of sharp edges and branching angles (Boyack & Ru, 2009). The spike points on AuNS serve as SERS hot-spots, intensifying the Raman signals of molecules that are bound to them. In addition to serving as SERS hot-spots, the sharp tips of nanostars also provide significantly large surface areas, enabling excellent interactions

between the substrate and analyte molecules. This, in turn, facilitates effective adsorption (Kumari & Singh, 2012).

The objective of this study was to investigate the feasibility of using SERS to simultaneously detect multiple pesticides on grape surfaces. As the use of multiple pesticides is common in the industry, detecting only one pesticide in food matrices at a time is insufficient. Therefore, there is an urgent need for on-site multi-pesticide detection techniques. SERS is a suitable technique for simultaneous multiplex detection due to its narrow Raman bands with minimal overlapping (Zhang et al., 2014). In this study, phosmet and paraquat, two pesticides, were artificially spiked to grape surfaces and simultaneously detected using AuNS as the SERS substrate, owing to their excellent SERS performance. The distinctive peaks of different pesticides can be easily used to differentiate each analyte in the mixture, enabling the detection of multiple pesticides through a single SERS measurement. This feature of the SERS technique can significantly reduce detection time and enhance efficiency.

4.2 Materials and Methods

4.2.1 Reagents, chemicals, and materials

Hydrogen tetrachloroaurate solution ($HAuCl_4$, 30 wt% in dilute HCl), trisodium citrate dihydrate (certified ACS), water (HPLC grade), and acetone (HPLC grade), were purchased from Fisher Scientific (Fair Lawn, New Jersey, USA). Paraquat (Pestanal® analytical standard), phosmet (Pestanal® analytical standard), 4-aminothiophenol (4-ATP), and hydroquinone were obtained from Sigma-Aldrich (St. Louis, MO, USA). For the experiments, analytical-grade reagents were exclusively used and obtained without any further processing. The grapes were sourced from a nearby Walmart, while the deionized

water utilized throughout the experiments had a resistivity of 18.2 MΩ cm^{-1} and met the Millipore Milli-Q grade standards. Prior to use, all glassware were soaked in aqua regia (HCl/HNO_3 3:1, v/v) for 24 h and rinsed with Milli-Q water.

4.2.2 Synthesis of seed solution

First, a 1% chloroauric acid solution (300 μL) was added to 30 mL of boiled deionized water in a flask, which was then subjected to stirring and heated until boiling again. Next, a 1% solution of sodium citrate (100 mL) was added to the above flask, and the resulting mixture was continuously stirred until it became a light red wine color. The heating was then terminated, but stirring was allowed to continue for an additional 30 min.

4.2.3 Growth solution for synthesis of AuNS

To prepare the AuNS, 25 μL of a 100 mM chloroauric acid solution was added to 10 mL of deionized water in a beaker, which was then stirred continuously. Next, 50 μL of a gold seed solution, 22 μL of a 1% sodium citrate solution, and 1 mL of a 30 mM hydroquinone solution were introduced to the above beaker, the color turned a light blue. The entire mixture was stirred at room temperature for 30 min to obtain AuNS. The solution containing AuNS was concentrated through centrifugation at 2705 rcf or 5500 rpm, and the supernatant was subsequently removed.

4.2.4 Characterization of AuNS

A UV-1099i spectrophotometer (Shimadzu, Kyoto, Japan) was used to measure the absorbance of gold seed solution at wavelengths between 400 and 700 nm with a cuvette filled with deionized water serving as the blank. To observe the shapes and determine the elemental composition of the AuNS, Thermo Scientific Spectra 300 (S)TEM coupled with the Super-X system was used to view the shape and analyze the elemental composition of

core-shell nanoparticles. An aliquot (5 μL) of Au/Ag solution was dropped on a copper grid prior and dried prior to the STEM analysis.

4.2.5 Preparation of standard solutions

To evaluate the enhancement of AuNS, various concentrations of 4-ATP ranging from 0.1, 0.5, 1, 5, and 10 mg/L were utilized as the Raman probe. To generate a calibration curve and determine the limit of detection, solutions of pesticides with varying concentrations were created via sequential dilution. Specifically, phosmet and paraquat powder were dissolved in acetone and water to form a standard stock solution with a concentration of 100 mg/L. Subsequently, this stock solution was diluted using deionized water to prepare pesticides with concentrations of 0.5, 1, 2, 5, 10, and 20 mg/L. To prepare mixtures of pesticides with varying concentration ratios, 1 mL of phosmet was mixed with 1 mL of paraquat at different concentrations.

4.2.6 Preparation of grapes sample

Clean grapes were peeled, and the resulting grape peels were cut into approximately 1-2 cm^2 in size. These peels were washed with water and soaked in water for 3 h before being dried with air and placed in a glass dish. Next, the grape peel was immersed in mixtures of pesticides with different concentrations for 24 h. The following day, the grape peels were left to evaporate at room temperature. The method used to extract pesticide molecules from the grape peels and enhance analyte concentration at the outer surface was based on the technique described by Bianhua Liu (Liu et al., 2012), Specifically, 10 μL of ethanol was applied to the sample surface and allowed to fully evaporate at room temperature. Next, 5 μL of concentrated AuNS solution was added to the contaminated grape peels and allowed to dry completely. To obtain blank data for the grape surface,

uncontaminated grape samples were treated with the same amount of ethanol and SERS substrate.

4.2.7 SERS measurements

SERS measurements were performed using a DXR2 Raman spectrometer (Thermo Fisher Scientific Inc., Waltham, MA, USA) equipped with a 785 nm laser source. The laser beam, with a power of 20 mW, was focused through a 10× objective lens, and a 25 μm pinhole aperture was used. Raman spectra were collected using OMNIC software (Thermo Fisher Scientific Inc.), and Raman measurements were taken from different locations of the samples with 10 scans per measurement and 3 s of exposure time per scan. To improve accuracy, ten measurements were averaged for each concentration of the samples.

4.2.8 Data analysis

Originlab (Originlab Corporation, Northampton, Massachusetts, United States) and Delight software (Delight, D-squared Development Inc., LaGrande, OR, USA) was utilized for Raman spectral analyses. The calibration curve was generated by plotting the SERS intensity against the analyte concentration (Sun et al., 2019). Each data point on the curve was calculated as an average value from ten replicate measurements. To calculate the analytical enhancement factor (AEF) of AuNS as a SERS substrate, 5 μL of the sample solution was deposited onto a spot of AuNS and a gold-coated glass slide. The AEF of the SERS method was determined using the following equation:

$$\mathrm{AEF} = I_{\mathrm{SERS}} / I_{\mathrm{RS}} \times C_{\mathrm{RS}} / C_{\mathrm{SERS}}$$

Where I_{SERS} and I_{RS} indicate the peak intensities in SERS and normal Raman spectra, respectively, and the analyte concentrations in SERS and normal Raman measurements are indicated by C_{SERS} and C_{RS}, respectively.

Partial Least Squares (PLS) analysis was also used in this study. Initially, the spectral data underwent preprocessing steps, including smoothing at a 2 cm^{-1} interval and a second-derivative transformation with a 12 cm^{-1} gap. These steps aimed to eliminate instrumental noises, separate overlapping peaks, and adjust the baseline shift to minimize spectral noise. Subsequently, PLS models were developed for the prediction of analyte concentrations. The correlation coefficient (*r*) was used as an indicator of the PLS model's accuracy in predicting analyte concentrations. The *r* ranges from 0 to 1, with values approaching 1 indicating a strong positive linear relationship. Each sample was subjected to ten replicate measurements, and the average value was utilized in the calibration plot. To calculate the root mean squared error of prediction (RMSEP), the following equation was employed. RMSEP is a commonly used measure of prediction error in statistical modeling.

$$\text{RMSEP}=\sqrt{\frac{\sum(y_i-\hat{y})^2}{n}}$$

4.3 Results and Discussion

4.3.1 Synthesis and characterization of AuNS

Gold nanostars (AuNS) were synthesized using a two-step seed-mediated growth method (Sun et al., 2019). Initially, chloroauric acid was reduced to form gold seeds in solution by adding a specific concentration of sodium citrate. Subsequently, in the growth solution, sodium citrate served as a reducing agent while hydroquinone acted as a morphological inducer. Despite sodium citrate's relatively weak reducing ability, it was still able to convert trivalent Au^{3+} to monovalent Au^{+} in the reaction system. The stronger reducing agent, hydroquinone, further reduced the monovalent Au^{+} to Au, resulting in the formation of 3D irregular star-shaped nanostructures (Sun et al., 2019). The seed solution

containing AuNS exhibited a ruby red color (Fig.4-1A) due to its ability to reflect red light and absorb green light. Unlike bulk gold, the color of gold nanoparticles can vary as their size and shape change. The presence of an absorption peak at approximately 521 nm in the UV-vis spectrum of the seed solution (Fig. 4-1B) signifies the plasmon resonance frequency exhibited by the gold nanoparticles. The peak with the highest absorbance in the seed solution can be used as a rapid indicator to verify the successful synthesis of the seed solution.

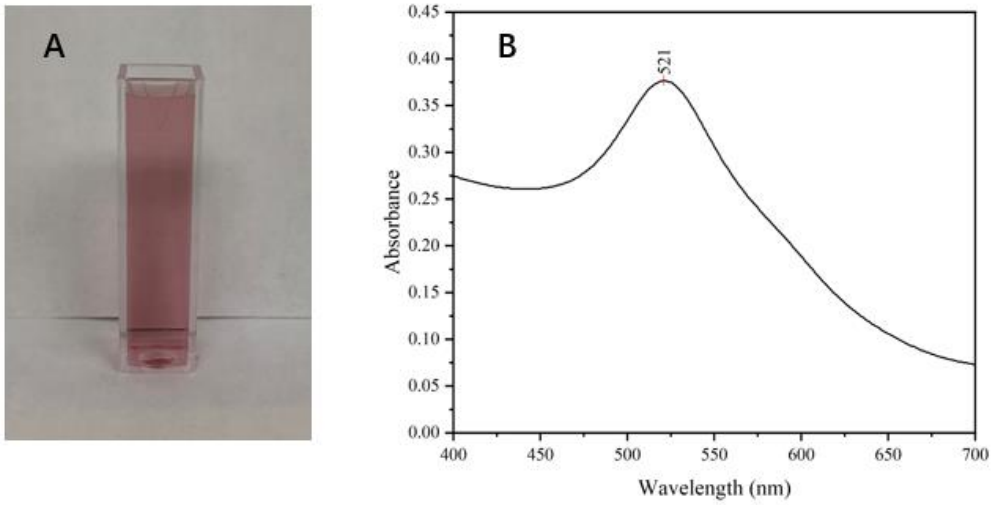

Figure 4-1 Seed solution for gold nanostars (A) and an UV–vis spectrum of the seed solution (B).

AuNS solution exhibits a blue color (Fig 4-2A), while its concentrated counterpart displays a deep blue color (Fig 4-2B). The synthesis process of AuNS entails the reduction of Au^{3+} to Au^{1+} by citrate, followed by the reduction of Au^{1+} to Au^{0} using hydroquinone. This sequential reduction selectively interacts with Au^{1+} ions, facilitating the formation of outwardly radiating branches (Li et al., 2011).

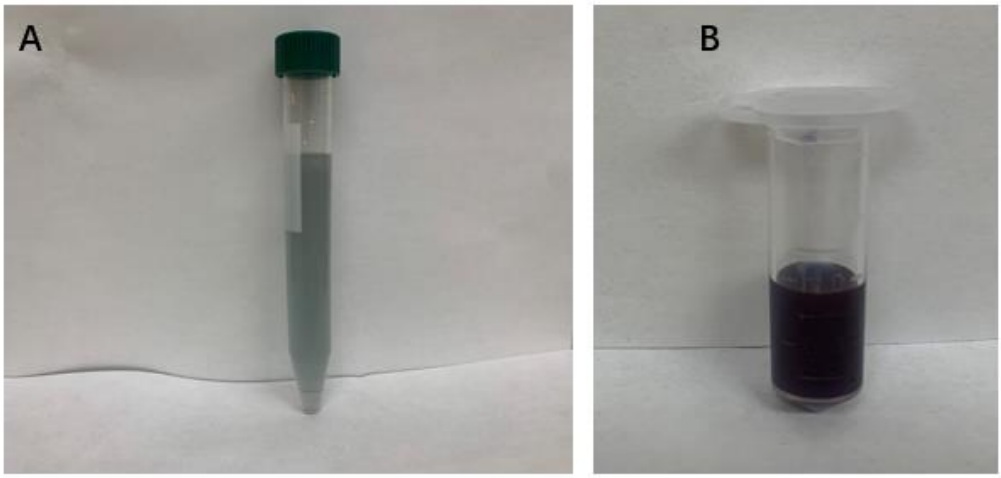

Figure 4-2 AuNS solution (A), concentrated AuNS solution (B).

Fig. 4-3 depicts complex 3D metal structures that exhibit non-symmetric and non-sharply- edged 3D nanostructures with a central core and multiple protruding branching angles. The size of the synthesized AuNS is consistently uniform, with an antenna size ranging from ~4 to 6 nm. The presence of these sharp edges and branching angles makes AuNS highly sensitive to local dielectric environments, exhibiting exceptional SERS effects.

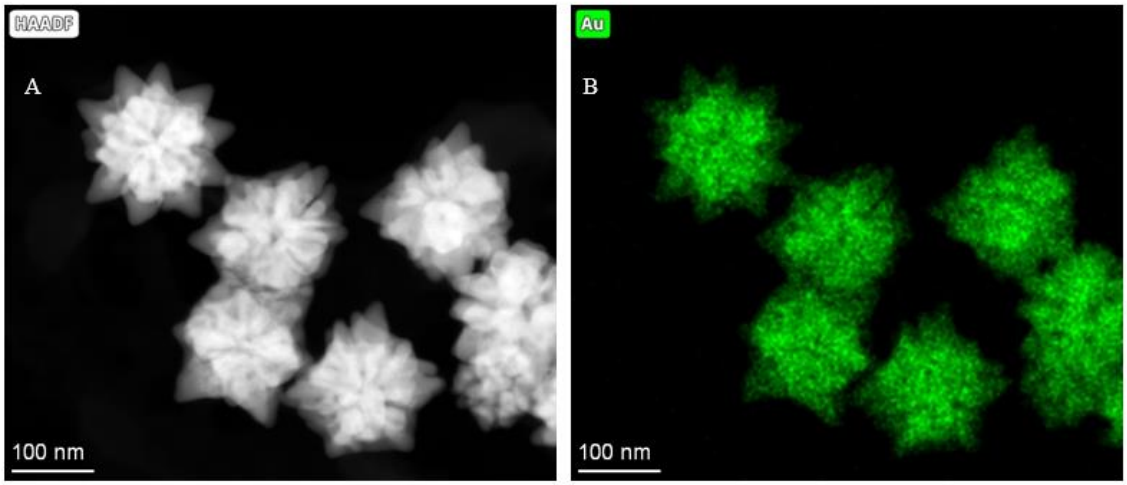

Figure 4-3 STEM image of gold nanostars (A) and the corresponding EDS image (B).

4.3.2 Evaluation of SERS performance of AUNS substrate

The performance of the synthesized AuNS was assessed in this study using 4-ATP as a Raman reporter. Previous studies have shown that 4-ATP is an effective probe molecule when combined with gold nanoparticles in SERS. For the SERS measurements conducted in this study, a range of 4-ATP solutions, ranging from 0.1 to 10 ppm, were intentionally selected. Fig 4-4 clearly shows SERS spectra (n = 10) in the wavelength range of 450-2000 cm^{-1}. The spectra of different concentrations of 4-ATP exhibit distinct differences, with two characteristic peaks observed at 1077 and 1579 cm^{-1}. Furthermore, there is a noticeable trend of increasing Raman intensity for both peaks at 1076 and 1583 cm^{-1}.

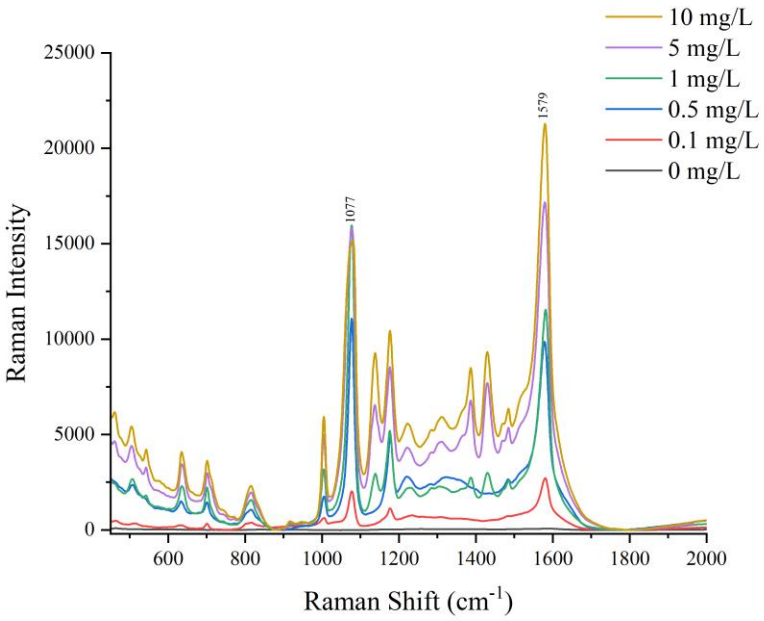

Figure 4-4 Raman spectra of 4-ATP obtained at different concentrations using the AuNS substrate.

4.3.3 SERS measurement of single pesticide, and their mixture, in water and on grapes

To get the characteristic Raman spectra of phosmet and paraquat, deposited two pesticide powders onto a gold-coated microscope slide and analyzed them using a Raman spectrometer. As shown in Figure 4-4, the range of 450 to 2000 cm^{-1} revealed over 4 characteristic peaks for paraquat and 7 peaks for phosmet. Raman spectra of paraquat, four significant characteristic peaks. These peaks correspond to the following vibrational modes: C–N stretching at 844 cm^{-1}, the C=N bending at 1202 cm^{-1}, the C–C structural distortion at 1303 cm^{-1}, and the C=N stretching at 1657 cm^{-1} (Lin et al., 2021). The Raman spectrum of phosmet revealed several significant bands related to various functional groups, including C=O, C-N, P-O-C, P=S, and C=C. Specifically, the peak at 504 cm^{-1} is associated with the rocking vibration of CH_2 and PO_2. In-plane deformation vibrations of C=O, P=S, and C-N were observed at approximately 607, 653, and 1192 cm^{-1}, respectively. The peak

at 715 cm^{-1} is likely attributed to vibrations of benzene rings, while the peak at 980 cm^{-1} can be linked to the asymmetric stretching of P-O-C. Additionally, the stretching of C=O was observed at 1775 cm^{-1} (Fan et al., 2014).

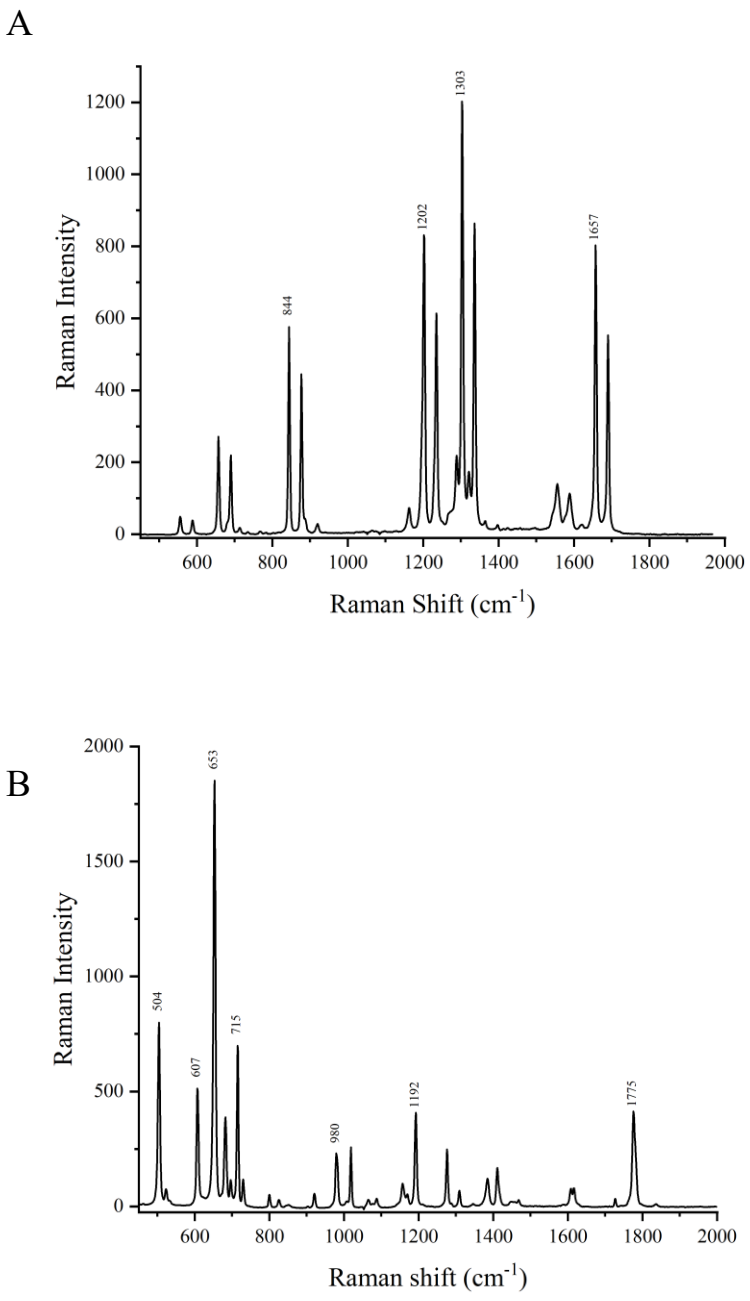

Figure 4-5 Raman spectra of pure paraquat (A) and phosmet (B) powders.

Figure 4-6 illustrates the average SERS spectra (n = 10) obtained for different concentrations of paraquat and phosmet solutions, ranging from 0.5 to 20 ppm. These spectra clearly exhibit enhanced Raman signals compared to those observed for pure powders of the two pesticides. The SERS peaks associated with paraquat (Figure 4-6A) are located at 834, 1011, 1184, and 1616 cm^{-1}, with the strongest peak observed at 1616 cm^{-1}. Furthermore, higher concentrations of paraquat lead to significantly increased Raman signals. Figure 4-6B presents the average (n = 10) SERS spectra of various concentrations of phosmet, showing distinctive Raman peaks at 499, 604, 783, 1013, 1190, and 1769 cm^{-1}. The intensity of these Raman peaks progressively augments as the phosmet concentration rises from 0 to 20 mg/L.

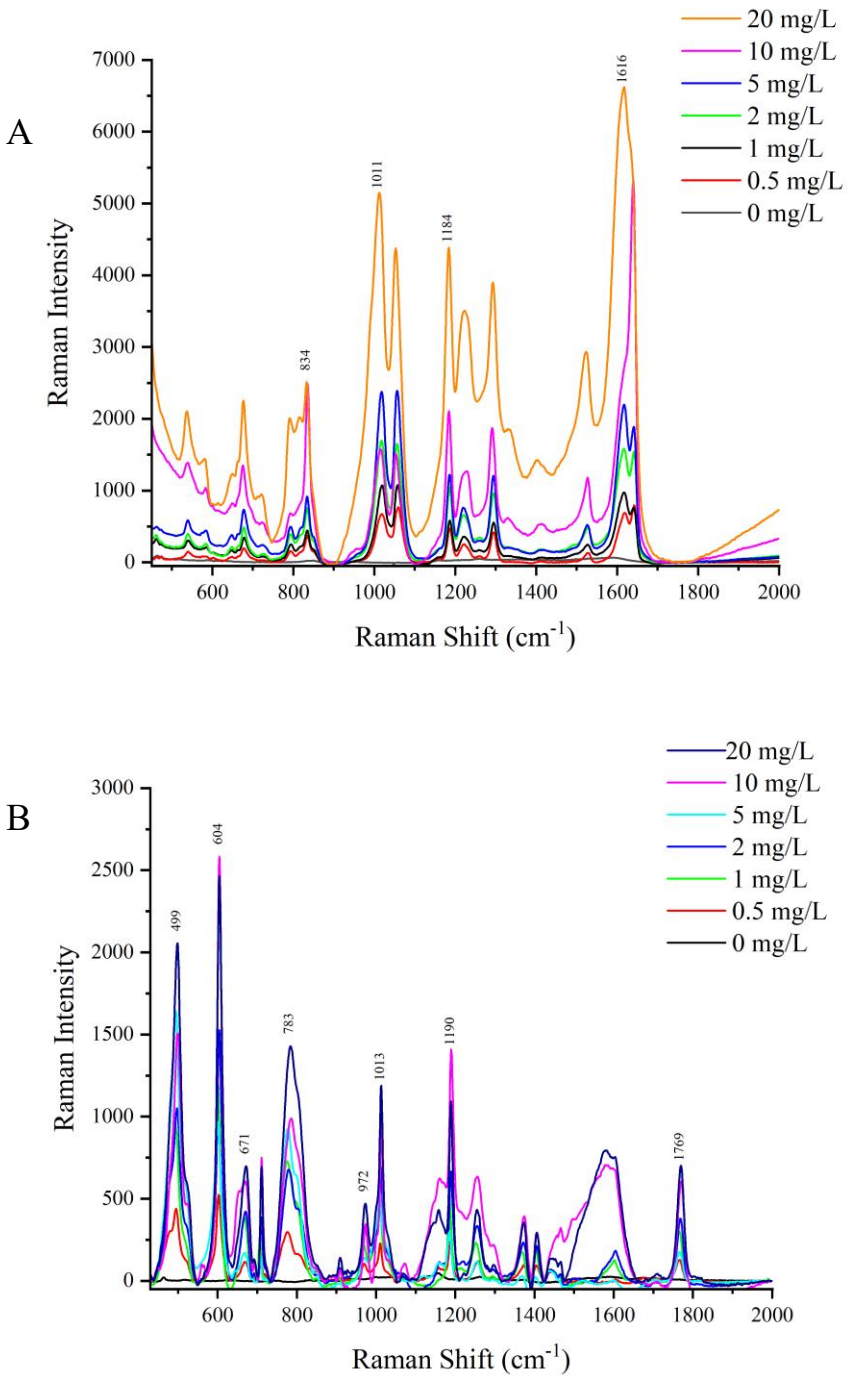

Figure 4-6 Average Raman spectra (n=10) of paraquat (A) and phosmet (B) at different concentration from 0.5 to 20 ppm.

Grapes, a non-climacteric type of fruit, are widely consumed worldwide and hold a long history of cultivation and enjoyment by humans for centuries (Wang et al., 2019). Available in an array of colors such as green, red, black, and purple, each variety carries a

distinctive flavor profile. Aside from their delicious taste, grapes also offer numerous health benefits. They can be enjoyed in various forms, including grape wine, juice, raisins, vinegar, or simply as table grapes. It's important to note, however, that grapes are classified among the "Dirty Dozen" foods due to their vulnerability to pests and diseases, which often necessitates the use of pesticides during cultivation (EWG, 2023). Throughout their growth cycle, conventionally grown grapes may be treated with different types of pesticides, including insecticides, fungicides, and herbicides. These pesticides have the potential to leave residues on the grape skin, which can be consumed when eaten.

Paraquat, a widely utilized herbicide, poses concerns for health and the environment as it disrupts the electron transfer of photosynthesis, leading to weed eradication (Sétif, 2015). Introduced in the 1960s, it gained popularity due to its cost-effectiveness and nonselective properties, making it applicable to a wide range of agricultural products (Huang et al., 2019). In certain countries, paraquat may be employed as an herbicide in grape cultivation to control weed growth. However, it is crucial to note that paraquat is highly toxic to humans, potentially causing pulmonary edema and harm to the heart, liver, and kidneys (Lin et al., 2021).

Another pesticide commonly used in agriculture is phosmet, an organophosphate insecticide, recognized for its ability to combat various pests that threaten crops, including aphids, caterpillars, mites, and leafhoppers (Biddinger et al., 2013). Phosmet functions by inhibiting acetylcholinesterase, thereby disrupting the nervous systems of insects and leading to paralysis, eventually resulting in their demise. Its application has been employed in grape cultivation to control these pests, which can pose damage to agricultural crop.

In aqueous solutions, Fig. 4-7A displays the SERS spectra of paraquat and phosmet mixture at different concentrations. The SERS peaks corresponding to phosmet are observed at 498, 605, 676, and 1767 cm^{-1}, while paraquat characteristic peaks at 836, 1014, 1188, and 1645 cm^{-1}. Furthermore, increasing concentrations of the mixture exhibit noticeably amplified Raman signals. In Figure 4-7B, the SERS spectra of different concentrations of a mixture on grapes are presented. The characteristic peaks observed in the spectra of grapes contaminated with phosmet or paraquat were similar to those of their respective standard solutions. The characteristic peaks of phosmet were observed at 495, 600, 670, and 1764 cm^{-1}, while those of paraquat were observed at 828, 1007, 1182, and 1632 cm^{-1}. These peaks showed slight shifts compared to the peaks in the Raman spectra of the standard solutions. By analyzing the characteristic peaks in the SERS spectra of grapes, the lowest concentration that could be detected was determined to be 0.5 mg/L for both pesticides.

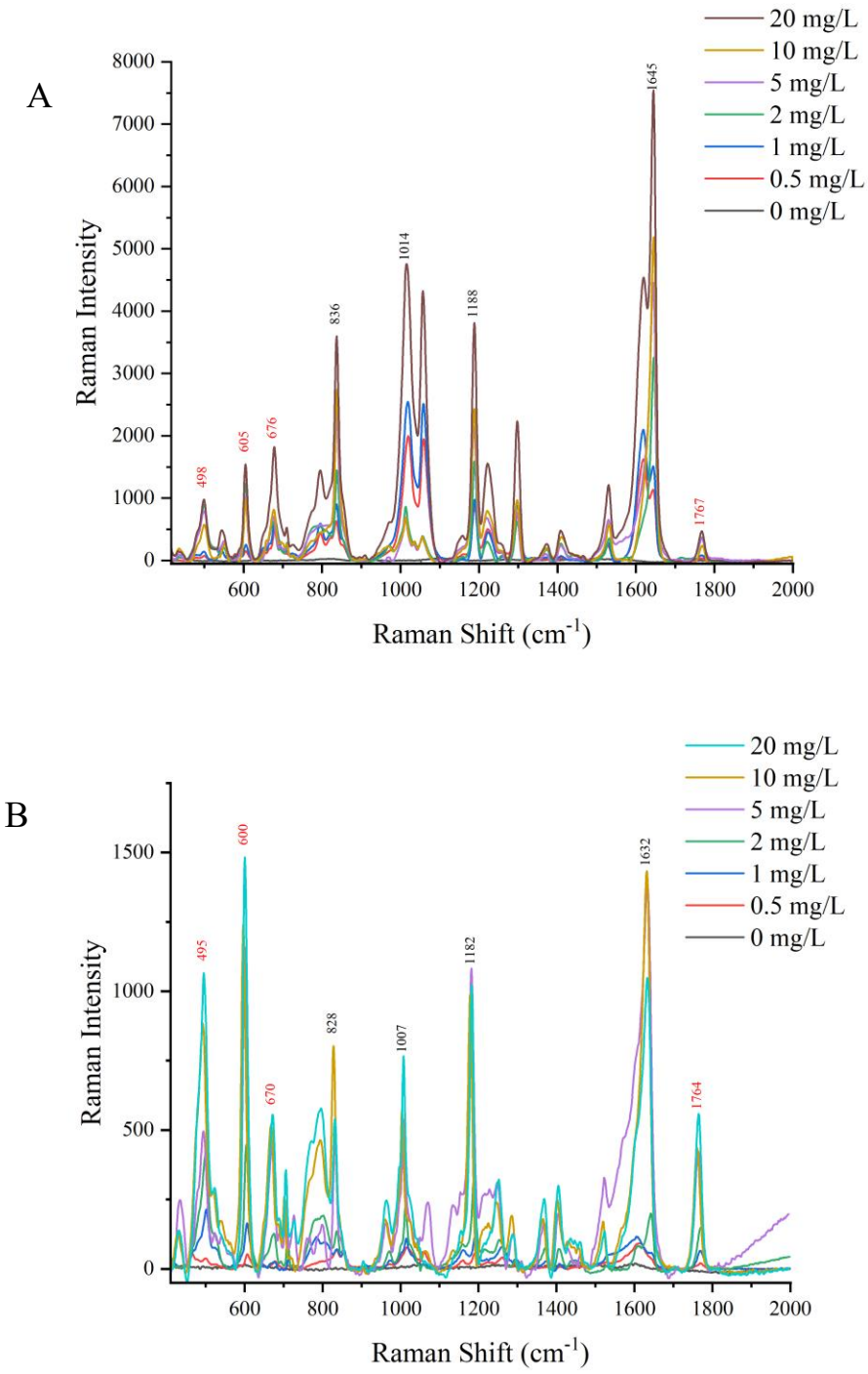

Figure 4-7 Averaged SERS spectra (n = 10) of mixture standard solutions (A); average SERS spectra (n = 10) of mixture on grapes.

This study focused on developing a PLS model to analyze SERS spectra of phosmet and paraquat, extracted from grapes. Fig. 4-8 illustrates the PLS models used to predict the concentrations of these two pesticides in the grape extract (n = 10), as shown by the calibration plots of spiked and predicted pesticide concentrations. Additionally, The R-value and RMSEP for the data are 0.90 and 2.94 mg/L, respectively (refer to Fig. 4-8). These results demonstrate the accuracy of the PLS model in predicting thiram and paraquat concentrations in the grape extract. Both pesticides exhibited high R values, indicating a robust linear correlation between the predicted and actual pesticide concentrations detected in the grape extract. The favorable linear relationship can be attributed to the well-structured and uniform nanocomposite substrate employed in the analysis.

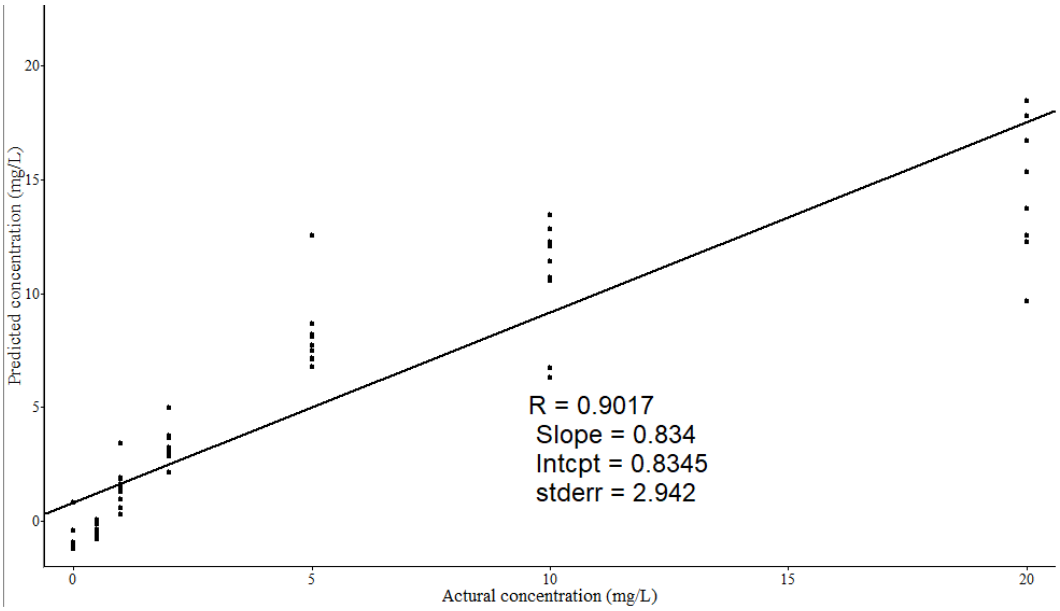

Figure 4-8 Predication of mixture pesticides concentration on grapes using the PLS model.

4.4 Summary

SERS is a promising alternative detection technique. In this study, the AuNS used were easily synthesized and provided significant enhancement effects for the Raman scattering signals of phosmet and paraquat. The method's detection limit for a phosmet-paraquat mixture on grapes was determined to be 0.5 mg/L. By utilizing PLS for SERS spectral data analysis, it was demonstrated that SERS technology has the potential for quantitative analysis. The satisfactory results obtained from this study conclude that the SERS method is rapid, effective, and shows great potential for qualifying and quantifying food contaminants. However, there is still room for optimizing the performance of SERS. Future studies can focus on developing approaches to orderly arrange AUNS and improving sample preparation techniques to achieve even lower detection limits while maintaining high Raman intensity.

CHAPTER 5

CONCLUSIONS AND FUTURE STUDY

Two research studies highlight SERS as a promising technique for detecting pesticides and food contaminants. The first study developed a reliable SERS substrate using Au/Ag NPs for analyzing a phosmet-paraquat mixture in green tea. It achieved exceptional performance, detecting the mixture at a low concentration of 0.1 mg/kg. The second study utilized easily synthesized AuNS to enhance Raman signals of phosmet and paraquat, achieving a 0.5 mg/L detection limit for grape samples. It demonstrated the potential of SERS for quantitative analysis of contaminants. Future efforts should focus on efficient AuNS arrangement and improved sample preparation to enhance detection limits while maintaining high Raman intensity.

Future studies in SERS for the detection of fresh produce offer substantial potential to enhance food safety and quality assessment. One avenue of exploration involves the development of optimized SERS substrates. Researchers can focus on designing substrates with tailored surface properties, nanoparticle shapes, and surface chemistries to amplify the SERS signal and improve detection sensitivity. By customizing the substrates for different types of fresh produce, specific and reliable detection methods can be established.

Another area of potential advancement lies in data analysis and machine learning techniques. Progress in these fields can greatly enhance the interpretation of complex SERS spectra obtained from fresh produce. By developing robust and reliable models, it becomes feasible to establish correlations between SERS data and quality parameters, identify potential hazards, and predict the freshness or spoilage of the produce (Zhou et al., 2023).

Leveraging data analysis and machine learning can provide valuable insights for quality control and enable more effective decision-making in the food industry.

Overall, the exploration of specialized SERS substrates and the integration of advanced data analysis techniques hold great promise for future advancements in the detection of fresh produce. These developments can significantly contribute to improving food safety, quality assessment, and ultimately benefit consumers and the food industry as a whole.

REFERENCES

Abd El-Aty, A. M., Choi, J.-H., Rahman, M. M., Kim, S.-W., Tosun, A., & Shim, J.-H. (2014). Residues and contaminants in tea and tea infusions: A review. *Food Additives & Contaminants. Part A, Chemistry, Analysis, Control, Exposure & Risk Assessment*, *31*(11), 1794–1804.

Altunbek, M., Kuku, G., & Culha, M. (2016). Gold Nanoparticles in Single-Cell Analysis for Surface Enhanced Raman Scattering. *Molecules*, *21*(12), 1617.

Asgari, S., Sun, L., Lin, J., Weng, Z., Wu, G., Zhang, Y., & Lin, M. (2020). Nanofibrillar cellulose/Au@Ag nanoparticle nanocomposite as a SERS substrate for detection of paraquat and thiram in lettuce. *Microchimica Acta*, *187*(7), 390.

Authority (EFSA), E. F. S., Medina-Pastor, P., & Triacchini, G. (2020). The 2018 European Union report on pesticide residues in food. *EFSA Journal*, *18*(4), e06057.

Awiaz, G., Lin, J., & Wu, A. (2023). Recent advances of Au@Ag core–shell SERS-based biosensors. *Exploration*, *3*(1), 20220072.

Bhattacharjee, G., Bhattacharya, M., Roy, A., Senapati, D., & Satpati, B. (2018). Core–Shell Gold@Silver Nanorods of Varying Length for High Surface-Enhanced Raman Scattering Enhancement. *ACS Applied Nano Materials*, *1*(10), 5589–5600.

Biddinger, D. J., Robertson, J. L., Mullin, C., Frazier, J., Ashcraft, S. A., Rajotte, E. G., Joshi, N. K., & Vaughn, M. (2013). Comparative Toxicities and Synergism of Apple Orchard Pesticides to Apis mellifera (L.) and Osmia cornifrons (Radoszkowski). *PLOS ONE*, *8*(9), e72587.

Boedeker, W., Watts, M., Clausing, P., & Marquez, E. (2020). The global distribution of acute unintentional pesticide poisoning: Estimations based on a systematic review. *BMC Public Health*, *20*(1), 1875.

Boyack, R., & Ru, E. C. L. (2009). Investigation of particle shape and size effects in SERS using T -matrix calculations. *Physical Chemistry Chemical Physics*, *11*(34), 7398–7405.

Chen, L., ShangGuan, L., Wu, Y., Xu, L., & Fu, F. (2012). Study on the residue and degradation of fluorine-containing pesticides in Oolong tea by using gas chromatography–mass spectrometry. *Food Control*, *25*(2), 433–440.

Chen, X., Wang, D., Li, J., Xu, T., Lai, K., Ding, Q., Lin, H., Sun, L., & Lin, M. (2020). A spectroscopic approach to detect and quantify phosmet residues in Oolong tea by surface-enhanced Raman scattering and silver nanoparticle substrate. *Food Chemistry*, *312*, 126016.

Cooper, J., & Dobson, H. (2007). The benefits of pesticides to mankind and the environment. *Crop Protection*, *26*(9), 1337–1348.

Costa, J. C. S., Ando, R. A., Sant'Ana, A. C., & Corio, P. (2012). Surface-enhanced Raman spectroscopy studies of organophosphorous model molecules and pesticides. *Physical Chemistry Chemical Physics*, *14*(45), 15645–15651.

C.V. Raman The Raman Effect—Landmark. (1998, December 15). American Chemical Society. https://www.acs.org/education/whatischemistry/landmarks/ramaneffect.html

Deriu, C., Thakur, S., Tammaro, O., & Fabris, L. (2023). Challenges and opportunities for SERS in the infrared: Materials and methods. *Nanoscale Advances*, *5*(8), 2132–2166.

Donno, D., Mellano, M. G., Gamba, G., Riondato, I., & Beccaro, G. L. (2020). Analytical Strategies for Fingerprinting of Antioxidants, Nutritional Substances, and Bioactive Compounds in Foodstuffs Based on High Performance Liquid Chromatography–Mass Spectrometry: An Overview. *Foods*, *9*(12), 1734.

Enhanced Elimination of Poisons—ClinicalKey. (n.d.). Retrieved February 25, 2023, from https://www.clinicalkey.com/#!/content/book/3-s2.0-B9780323532655000678

EWG. (2023, March 15). *EWG's 2023 Shopper's Guide to Pesticides in Produce™*. https://www.ewg.org/foodnews/summary.php

Fan, Y., Lai, K., Rasco, B. A., & Huang, Y. (2014). Analyses of phosmet residues in apples with surface-enhanced Raman spectroscopy. *Food Control*, *37*, 153–157.

Food safety. (2022, May 19). https://www.who.int/news-room/fact-sheets/detail/food-safety

Ghosh Chaudhuri, R., & Paria, S. (2012). Core/Shell Nanoparticles: Classes, Properties, Synthesis Mechanisms, Characterization, and Applications. *Chemical Reviews*, *112*(4), 2373–2433.

Good, J. L., Khurana, R. K., Mayer, R. F., Cintra, W. M., & Albuquerque, E. X. (1993). Pathophysiological studies of neuromuscular function in subacute organophosphate poisoning induced by phosmet. *Journal of Neurology, Neurosurgery, and Psychiatry*, *56*(3), 290–294.

Harris, D. C., & Bertolucci, M. D. (1989). *Symmetry and spectroscopy: An introduction to vibrational and electronic spectroscopy*. Dover Publications.

Hassing, S. (2019). What Is Vibrational Raman Spectroscopy: A Vibrational or an Electronic Spectroscopic Technique or Both? In *Modern Spectroscopic Techniques and Applications*. IntechOpen.

Haynes, C. L., McFarland, A. D., & Van Duyne, R. P. (2005). Surface-Enhanced Raman Spectroscopy. *Analytical Chemistry*, *77*(17), 338 A-346 A.

Hu, X., Wang, T., Wang, L., & Dong, S. (2007). Surface-Enhanced Raman Scattering of 4-Aminothiophenol Self-Assembled Monolayers in Sandwich Structure with Nanoparticle Shape Dependence: Off-Surface Plasmon Resonance Condition. *The Journal of Physical Chemistry C*, *111*(19), 6962–6969.

Huang, Y., Zhan, H., Bhatt, P., & Chen, S. (2019). Paraquat Degradation From Contaminated Environments: Current Achievements and Perspectives. *Frontiers in Microbiology*, *10*. https://www.frontiersin.org/articles/10.3389/fmicb.2019.01754

Hutter, E., & Fendler, J. H. (2004). Exploitation of Localized Surface Plasmon Resonance. *Advanced Materials*, *16*(19), 1685–1706.

Kim, S.-H., Oh, S. S., Kim, K.-J., Kim, J.-E., Park, H. Y., Hess, O., & Kee, C.-S. (2015). Subwavelength localization and toroidal dipole moment of spoof surface plasmon polaritons. *Physical Review B*, *91*(3), 035116.

Kumari, S., & Singh, R. P. (2012). Glycolic acid-g-chitosan-gold nanoflower nanocomposite scaffolds for drug delivery and tissue engineering. *International Journal of Biological Macromolecules*, *50*(3), 878–883.

Langley, R. L., & Mort, S. A. (2012). Human Exposures to Pesticides in the United States. *Journal of Agromedicine*, *17*(3), 300–315.

Li, D.-W., Zhai, W.-L., Li, Y.-T., & Long, Y.-T. (2014). Recent progress in surface enhanced Raman spectroscopy for the detection of environmental pollutants. *Microchimica Acta*, *181*(1), 23–43.

Li, J., Wu, J., Zhang, X., Liu, Y., Zhou, D., Sun, H., Zhang, H., & Yang, B. (2011). Controllable Synthesis of Stable Urchin-like Gold Nanoparticles Using Hydroquinone to Tune the Reactivity of Gold Chloride. *The Journal of Physical Chemistry C*, *115*(9), 3630–3637.

Li, W., Guo, Y., & Zhang, P. (2010). SERS-Active Silver Nanoparticles Prepared by a Simple and Green Method. *The Journal of Physical Chemistry C*, *114*(14), 6413–6417.

Lin, M.-H., Sun, L., Kong, F., & Lin, M. (2021). Rapid detection of paraquat residues in green tea using surface-enhanced Raman spectroscopy (SERS) coupled with gold nanostars. *Food Control*, *130*, 108280.

Liu, B., Han, G., Zhang, Z., Liu, R., Jiang, C., Wang, S., & Han, M.-Y. (2012). Shell Thickness-Dependent Raman Enhancement for Rapid Identification and Detection of Pesticide Residues at Fruit Peels. *Analytical Chemistry*, *84*(1), 255–261.

Liu, B., Zhou, P., Liu, X., Sun, X., Li, H., & Lin, M. (2013). Detection of Pesticides in Fruits by Surface-Enhanced Raman Spectroscopy Coupled with Gold Nanostructures. *Food and Bioprocess Technology*, *6*(3), 710–718.

Lock, E. A., & Wilks, M. F. (2001). CHAPTER 70—Paraquat. In R. I. Krieger & W. C. Krieger (Eds.), *Handbook of Pesticide Toxicology (Second Edition)* (pp. 1559–1603). Academic Press.

Loiseau, A., Asila, V., Boitel-Aullen, G., Lam, M., Salmain, M., & Boujday, S. (2019). Silver-Based Plasmonic Nanoparticles for and Their Use in Biosensing. *Biosensors*, *9*(2), 78.

Lu, X., Rycenga, M., Skrabalak, S. E., Wiley, B., & Xia, Y. (2009). Chemical synthesis of novel plasmonic nanoparticles. *Annual Review of Physical Chemistry*, *60*, 167–192.

Luo, H., Huang, Y., Lai, K., Rasco, B. A., & Fan, Y. (2016). Surface-enhanced Raman spectroscopy coupled with gold nanoparticles for rapid detection of phosmet and thiabendazole residues in apples. *Food Control*, *68*, 229–235.

Luo, H., Wang, X., Huang, Y., Lai, K., Rasco, B. A., & Fan, Y. (2018). Rapid and sensitive surface-enhanced Raman spectroscopy (SERS) method combined with gold nanoparticles for determination of paraquat in apple juice. *Journal of the Science of Food and Agriculture*, *98*(10), 3892–3898.

Mulvihill, M., Tao, A., Benjauthrit, K., Arnold, J., & Yang, P. (2008). Surface-Enhanced Raman Spectroscopy for Trace Arsenic Detection in Contaminated Water. *Angewandte Chemie International Edition*, *47*(34), 6456–6460.

Narenderan, S. T., Meyyanathan, S. N., & Babu, B. (2020). Review of pesticide residue analysis in fruits and vegetables. Pre-treatment, extraction and detection techniques. *Food Research International*, *133*, 109141.

Njoki, P. N., Lim, I.-I. S., Mott, D., Park, H.-Y., Khan, B., Mishra, S., Sujakumar, R., Luo, J., & Zhong, C.-J. (2007). Size Correlation of Optical and Spectroscopic Properties for Gold Nanoparticles. *The Journal of Physical Chemistry C*, *111*(40), 14664–14669.

Ntzani, E. E., Ntritsos G, C. M., Evangelou, E., & Tzoulaki, I. (2013). Literature review on epidemiological studies linking exposure to pesticides and health effects. *EFSA Supporting Publications*, *10*(10), 497E.

Panigrahi, S., Basu, S., Praharaj, S., Pande, S., Jana, S., Pal, A., Ghosh, S. K., & Pal, T. (2007). Synthesis and Size-Selective Catalysis by Supported Gold Nanoparticles: Study on Heterogeneous and Homogeneous Catalytic Process. *The Journal of Physical Chemistry C*, *111*(12), 4596–4605.

Park, Y., Im, H., Weissleder, R., & Lee, H. (2015). Nanostar clustering improves the sensitivity of plasmonic assays. *Bioconjugate Chemistry*, *26*(8), 1470–1474.

Pesticides & Human Health | Californians for Pesticide Reform. (n.d.). Retrieved March 6, 2023, from https://www.pesticidereform.org/pesticides-human-health/

Pilot, R., Signorini, R., Durante, C., Orian, L., Bhamidipati, M., & Fabris, L. (2019). A Review on Surface-Enhanced Raman Scattering. *Biosensors*, *9*(2), 57.

Radziuk, D., & Moehwald, H. (2015). Prospects for plasmonic hot spots in single molecule SERS towards the chemical imaging of live cells. *Physical Chemistry Chemical Physics*, *17*(33), 21072–21093.

Reddy, D., & Colman, E. (2017). A Comparative Toxidrome Analysis of Human Organophosphate and Nerve Agent Poisonings Using Social Media. *Clinical and Translational Science*, *10*(3), 225–230.

Saito-Shida, S., Hamasaka, T., Nemoto, S., & Akiyama, H. (2018). Multiresidue determination of pesticides in tea by liquid chromatography-high-resolution mass spectrometry: Comparison between Orbitrap and time-of-flight mass analyzers. *Food Chemistry*, *256*, 140–148.

Sétif, P. (2015). Electron-transfer kinetics in cyanobacterial cells: Methyl viologen is a poor inhibitor of linear electron flow. *Biochimica et Biophysica Acta (BBA) - Bioenergetics*, *1847*(2), 212–222.

Shackman, H. M., Ding, W., & Bolgar, M. S. (2015). A Novel Route to Recognizing Quaternary Ammonium Cations Using Electrospray Mass Spectrometry. *Journal of the American Society for Mass Spectrometry*, *26*(1), 181–189.

Sharma, B., Frontiera, R. R., Henry, A.-I., Ringe, E., & Van Duyne, R. P. (2012). SERS: Materials, applications, and the future. *Materials Today*, *15*(1), 16–25.

Sinnathurai, S. (2023, June 30). *Tea | Definition, Types, & History | Britannica*. https://www.britannica.com/topic/tea-beverage

Stamplecoskie, K. G., Scaiano, J. C., Tiwari, V. S., & Anis, H. (2011). Optimal Size of Silver Nanoparticles for Surface-Enhanced Raman Spectroscopy. *The Journal of Physical Chemistry C*, *115*(5), 1403–1409.

Stöckle, R. M., Suh, Y. D., Deckert, V., & Zenobi, R. (2000). Nanoscale chemical analysis by tip-enhanced Raman spectroscopy. *Chemical Physics Letters*, *318*(1), 131–136.

Sun, L., Chen, P., & Lin, L. (2016). *Enhanced Molecular Spectroscopy via Localized Surface Plasmon Resonance* (M. T. Stauffer, Ed.). InTech.

Sun, L., Yu, Z., & Lin, M. (2019). Synthesis of polyhedral gold nanostars as surface-enhanced Raman spectroscopy substrates for measurement of thiram in peach juice. *Analyst*, *144*(16), 4820–4825.

Wang, K., Sun, D.-W., Pu, H., & Wei, Q. (2019). Surface-enhanced Raman scattering of core-shell Au@Ag nanoparticles aggregates for rapid detection of difenoconazole in grapes. *Talanta*, *191*, 449–456.

Williams, P. C., & Sobering, D. C. (1993). Comparison of Commercial near Infrared Transmittance and Reflectance Instruments for Analysis of Whole Grains and Seeds. *Journal of Near Infrared Spectroscopy*, *1*(1), 25–32.

Xie, W., Su, L., Donfack, P., Shen, A., Zhou, X., Sackmann, M., Materny, A., & Hu, J. (2009). Synthesis of gold nanopeanuts by citrate reduction of gold chloride on gold–silver core–shell nanoparticles. *Chemical Communications*, *0*(35), 5263–5265.

Xu, M.-L., Gao, Y., Han, X.-X., & Zhao, B. (2022). Innovative Application of SERS in Food Quality and Safety: A Brief Review of Recent Trends. *Foods*, *11*(14), 2097.

Xu, X., Li, H., Hasan, D., Ruoff, R. S., Wang, A. X., & Fan, D. L. (2013). Near-Field Enhanced Plasmonic-Magnetic Bifunctional Nanotubes for Single Cell Bioanalysis. *Advanced Functional Materials*, *23*(35), 4332–4338.

Yilmaz, A., & Yilmaz, M. (2020). Bimetallic Core–Shell Nanoparticles of Gold and Silver via Bioinspired Polydopamine Layer as Surface-Enhanced Raman Spectroscopy (SERS) Platform. *Nanomaterials*, *10*(4), 688.

Zhang, X., Mobley, N., Zhang, J., Zheng, X., Lu, L., Ragin, O., & Smith, C. J. (2010). Analysis of agricultural residues on tea using d-SPE sample preparation with GC-

NCI-MS and UHPLC-MS/MS. *Journal of Agricultural and Food Chemistry*, *58*(22), 11553–11560.

Zhang, Y., Wang, Z., Wu, L., Pei, Y., Chen, P., & Cui, Y. (2014). Rapid simultaneous detection of multi-pesticide residues on apple using SERS technique. *Analyst*, *139*(20), 5148–5154.

Zhou, H., Xu, L., Ren, Z., Zhu, J., & Lee, C. (2023). Machine learning-augmented surface-enhanced spectroscopy toward next-generation molecular diagnostics. *Nanoscale Advances*, *5*(3), 538–570.

VITA

Kairui Zhai, born on October 18, 1996, hails from Changji, Xinjiang, China. He completed his Bachelor of Science degree in Nutrition and Exercise Physiology at the University of Missouri. During his junior year, he actively participated in various research programs. Additionally, he worked as a researcher at a Veterinary Diagnostic Lab, where he gained hands-on experience utilizing HPLC and LC-MS for the identification, quantification, and toxic analysis of ergot and ergovaline in plants and animal feed. Following his graduation, he decided to pursue a master's degree in Food Science at the University of Missouri, starting in Fall 2021. It was during this program that he began his exploration of SERS technology.